



NEAR EAST UNIVERSITY

INSTITUTE OF GRADUATE STUDIES

DEPARTMENT OF ANALYTICAL CHEMISTRY

**DETERMINATION OF IODATE IN TABLE SALT BY DEEP EUTECTIC
SOLVENT LIQUID-LIQUID MICROEXTRACTION PRIOR TO
SMARTPHONE DIGITAL IMAGE COLORIMETRY**

M.Sc. THESIS

Calvin Michan Olabodae VENN

Nicosia

January 2023

NEAR EAST UNIVERSITY
INSTITUTE OF GRADUATE STUDIES
DEPARTMENT OF ANALYTICAL CHEMISTRY

**DETERMINATION OF IODATE IN TABLE SALT BY DEEP EUTECTIC
SOLVENT LIQUID-LIQUID MICROEXTRACTION PRIOR TO
SMARTPHONE DIGITAL IMAGE COLORIMETRY**

M.Sc. THESIS

Calvin Michan Olabodae VENN

Supervisor

Dr. Jude Joshua Caleb

Co-Supervisor




Asst. Prof. Dr. Victor Markus

Nicosia

January, 2023

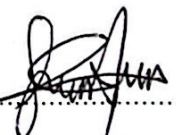
Approval

We certify that we have read the thesis submitted by Calvin Michan Olabodae VENN titled “**determination of iodate in table salt by deep eutectic solvent liquid-liquid microextraction prior to smartphone digital image colorimetry**” and in our combined opinion is fully adequate, in scope and in quality, as a thesis for the degree of Master of Analytical Chemistry.

Examining Committee	Name-Surname	Signature
Head of the Committee:	Assist Prof. Dr. Selin Isik	
Committee Member:	Dr. Mais Al-Nidawi	
Supervisor:	Dr. Jude Caleb	

Approved by the Head of the Department

30.01/2023



Assist. Prof. Dr. Selin Isik

Head of Department

Approved by the Institute of Graduate Studies

Prof. Dr. Kemal Husnu Can Baser
Head of the Institute

30.01/2023



Declaration

I forthwith declare that all information, documents, experimental and statistical analysis, and results in this thesis have been collected, done, and presented according to the academic rules and ethical guidelines of the Institute of Graduate Studies, Near East University.

I also hereby declare that as required by these rules and conduct, I have fully cited and referenced information and data that are not original to this study.

Calvin Michan Olabodae Venn

13/01/2023

Acknowledgements

Praise of praise our God and king, Hymns of adoration sing. For his mercies aye endure, ever faithful ever sure. To God Almighty I give all the glory with a heart full of praise and thanksgiving for seeing me through this chapter of my life.

My immense and profound gratitude goes to my course advisor and thesis supervisor, Dr. Jude Joshua Caleb, who has been a phenomenal lecturer, constant guide, and inspiration. In him I found a mentor and a friend.

An extension of my profound gratitude goes to my co-supervisor Asst. Prof. Dr. Victor Markus. Thank you for the imparted knowledge, sir.

I would like to extend my gratitude to my head of department Dr. Selin Isik and to Dr. Mais Al-Nidawi, of the department of analytical chemistry for their kind support throughout this process.

A very special thanks to Asst. Prof. Dr. Usama Alshana who officially introduced me to the beauty of analytical chemistry. In deep gratitude for your guidance, sir.

I am forever grateful to my father, Mr. Cecil Michael Olatunji Venn, for his unending support and encouragement. Thank you for being there Dad.

To my mother, Miss Christiana Olushola Fraser, your prayers and love kept me pushing. Thank you, Mum. And to my sister, Jeanne Albertina Regina Ganda, thank you for your constant support.

To my family and friends here in TRNC (Mrs. Isata Koroma, Ibrahim Dumbuya) home and abroad I say a big thanks for all the love and prayers.

Dedication

This work is dedicated to the two bundles of joy and love in my life, my son Cameron Mathew Oladiran Venn and my daughter, Camrene Madeline Olayinka Venn.

In fond memories of my late grandparents, Mr. & Mrs. Cecil Lewis Omotunde Venn, and Mr. & Mrs. Olabodae Fraser.

Abstract

Determination of Iodate in Table Salt by Deep Eutectic Solvent Liquid-Liquid Microextraction Prior to Smartphone Digital Image Colorimetry

Venn, Calvin Michan Olabodae

M.Sc., Department of Analytical Chemistry

Supervisor: Dr. Jude Joshua Caleb

January 2023, 68 Pages

In this study, the quantitative investigation of iodate in table salt by combining a green extraction technique with a unique and simple detection system is proposed. Deep eutectic solvent liquid-liquid microextraction (DES-LLME) method is combined with smartphone digital image colorimetry (SDIC) for the quantitative determination of iodate in table salt.

To capture reproducible images of the redox-enabled samples, an aluminum colorimetric box was built in-house. To achieve optimum conditions for the proposed system, parameters influencing the performance of both the DES-LLME and SDIC techniques were fine-tuned. The volume of DES (1000 μL), molar ratio of the DES (1:5), and the impact of an emulsifying agent are all optimal conditions for the DES-LLME that were studied.

A $0.6 \mu\text{g g}^{-1}$ concentration was determined as the lowest quantified concentration (LOD) of the proposed system with an Enrichment factor of 12.0. A correlation of concentration and absorbance exhibiting satisfactory proportion (linearity), thus demonstrating a well-fitted regression model ($R^2 = 0.9992$) was attained. Percentage relative standard deviation (%RSD) was obtained below 5.9% with good Intraday and Interday precision at 2.2 and 5.5 respectively.

Keywords: Smartphone digital image colorimetry, optimization, deep eutectic solvents, liquid-liquid microextraction, images, channel.

Öz

Akıllı Telefon Dijital Görüntü Kolorimetrisi Öncesinde Derin Ötektik Çözücü Sıvı-Sıvı Mikro Ekstraksiyonu ile Sofra Tuzundaki İyoda Tayini

Venn, Calvin Michan Olabodae

Yüksek Lisans, Analitik Kimya Anabilim Dalı

Danışman: Dr. Jude Joshua Caleb

Ocak 2023, 68 Sayfa

Bu çalışmada, yeşil bir ekstraksiyon tekniği ile benzersiz ve basit bir tespit sistemi birleştirilerek sofrta tuzundaki iyodatın niceliksel olarak araştırılması önerilmiştir. Derin ötektik çözücü sıvı-sıvı mikroekstraksiyon (DES-LLME) yöntemi, sofrta tuzundaki iyodat miktarının belirlenmesi için akıllı telefon dijital görüntü kolorimetrisi (SDIC) ile beraber kullanılmıştır.

Redoks özellikli örneklerin tekrarlanabilir görüntülerini yakalamak için sistem içi bir alüminyum kolorimetrik kutu yapılmıştır. Uygulanan sistemde optimum koşulları elde etmek için, hem DES-LLME hem de SDIC tekniklerinin performansını etkileyen parametreler ayarlanmıştır. DES-LLME için en uygun koşullar DES'in hacmi (1000 µL), DES'in molar oranı (1:5) ve bir emülsifiye edici maddenin etkisi için belirlenmiştir.

0,6 µg g⁻¹ konsantrasyonu, 12,0'lik iyileştirme faktörü ile önerilen sistemin en düşük nicel konsantrasyonu (LOD) olarak belirlenmiştir. Anlamlı bir oran (doğrusallık) sergileyen, dolayısıyla uyumlu bir regresyon modeli ($R^2 = 0.9992$) gösteren bir konsantrasyon ve absorbans korelasyonu elde edilmiştir. Yüzdelerik bağıl standart sapma (%RSD), sırasıyla 2,2 ve 5,5 olarak gün içi ve gün arası duyarlılık ile ölçülmüş ve %5,9'un altında elde edilmiştir.

Anahtar Kelimeler: Akıllı telefon dijital görüntü kolorimetrisi, optimizasyon, derin ötektik çözücüler, sıvı-sıvı mikro ekstraksiyon, görüntüler, kanal.

Table Of Contents

APPROVAL	1
DECLARATION	2
ACKNOWLEDGEMENTS	3
DEDICATION	4
ABSTRACT	5
ÖZ	6
TABLE OF CONTENTS	7
LIST OF FIGURES	10
LIST OF TABLES	11
LIST OF ABBREVIATIONS	12
CHAPTER I	14
INTRODUCTION	14
BENEFITS OF IODIZED TABLE SALTS	15
<i>Healthy Pregnancy Support</i>	15
<i>Healthy Heart Promotion and Hydration</i>	15
<i>Boost Thyroid Function</i>	15
<i>Toxins and Bacteria Removal and Prevention</i>	16
SOURCES OF IODINE AND SALT IODIZATION	16
RECOMMENDED INTAKE OF IODINE	16
IODINE DEFICIENCY	17
IMPACT OF HIGH IODINE INTAKE	17
HIGHLIGHT OF THE PROBLEM	18
OBJECTIVE OF THE STUDY	18
RESEARCH QUESTIONS AND HYPOTHESIS	18
SIGNIFICANCE OF THE STUDY	19
CHAPTER II	20
LITERATURE REVIEW	20
THEORETICAL FRAMEWORK	20

DEEP EUTECTIC SOLVENTS	20
<i>Synthesis Of DES</i>	22
<i>Classes of DES</i>	23
<i>Physicochemical Properties of DES</i>	24
Freezing Point.	24
Viscosity.	25
Density.	26
Polarity.....	27
DEEP EUTECTIC SOLVENTS IN MICROEXTRACTION.....	28
<i>Deep Eutectic Solvent as Extraction Solvent in Liquid-Liquid Micro-Extraction</i>	28
DIGITAL IMAGE COLORIMETRY ON A SMARTPHONE	30
<i>Assembling of the Colorimetric Detection System</i>	32
<i>Optimized Parameters of the SDIC System</i>	33
Wavelength of the Single Line (Monochromatic) Light Source.	33
Preferred Red, Green, Blue Channel.....	34
Optimal distance Between Detection Camera and Sample Solution.	35
Specified Area for Measurement (ROI).....	36
Signal Conversion.	36
Converting Signal into Concentration.	37
THE ANALYTE.....	38
<i>Iodate</i>	38
CHAPTER III	39
MATERIALS AND METHODS.....	39
CONSUMABLES	39
APPARATUS.....	39
STATISTICAL ANALYSIS	40
SAMPLE PREPARATION.....	40
PREPARATION OF SOLUTIONS.....	41
<i>Stock Solution</i>	41
<i>Potassium Iodide Solution</i>	41
<i>Preparation of 1M HCl Solution</i>	41
<i>Preparation of Salt Sample Solution</i>	41

REDOX REACTION FOR IODATE QUANTITATION IN TABLE SALT.....	41
SYNTHESIS OF THE DEEP EUTECTIC SOLVENT (DES).....	42
REACTION PROCEDURE.....	43
SIGNAL CONVERSION.....	44
CHAPTER IV.....	46
RESULTS AND DISCUSSION.....	46
DETERMINATION OF IODATE IN TABLE SALT BY DEEP EUTECTIC SOLVENT LIQUID- LIQUID MICRO-EXTRACTION PRIOR TO SMARTPHONE DIGITAL IMAGE	
COLORIMETRY.....	46
<i>Optimization of The Deep Eutectic Solvent Conditions</i>	46
Molar Ratio of the DES.....	46
Volume of the DES.....	47
Emulsifying Agent.....	47
<i>Optimization of Parameters of the SDIC System</i>	48
Construction of the Detection Box.....	48
Selection of the RGB Channel.....	49
Optimal Length Between Detection Camera and Sample Solution.....	50
Specified Area of Measurement (ROI).....	51
ANALYTICAL PERFORMANCE OF THE DEEP EUTECTIC SOLVENT LIQUID-LIQUID MICRO-EXTRACTION.....	52
DETERMINED CONCENTRATIONS OF THE IODIZED TABLE SALT SAMPLES.....	54
EVALUATION OF THE DEVELOPED METHOD TO OTHER TECHNIQUES.....	55
CHAPTER V.....	57
CONCLUSIONS AND RECOMMENDATIONS.....	57
REFERENCES.....	58

List Of Figures

Figure 1. The Evolution of DES Within the Last Decade	23
Figure 2. Applications of the Green Solvent (DES) in Liquid-Liquid Microextraction	30
Figure 3. Configuration of an Optic System	32
Figure 4. Colorimetric Box	33
Figure 5. Selection of RGB Channel	35
Figure 6. Highlighting the Region of Interest	36
Figure 7. Signal Conversion	37
Figure 8. Simplified Diagram of the Redox Reaction	42
Figure 9. Synthesis of the Deep Eutectic Solvent.....	43
Figure 10. Schematic Diagram of DESLLME.....	44
Figure 11. Proposed SDIC System	45
Figure 12. Selection of the DES Molar Ratio	46
Figure 13. Selection of Volume of DES	47
Figure 14. Study of the use of emulsifying solvent	48
Figure 15. Schematic Diagram of the Colorimetric System	49
Figure 16. RGB Channel Selection.....	50
Figure 17. Optimal Distance Between Detection Camera and Sample Solution.....	51
Figure 18. Specified Region of Interest (ROI).....	52

List Of Tables

Table 1. General Formula for the Formation of DES	24
Table 2. Freezing Points of Some Common DES.....	25
Table 3. Viscosities of some common DES.....	26
Table 4. Densities of some Common DES	27
Table 5. DES-LLME-SDIC Figures of Merit for Iodate Determination	53
Table 6. Determined Concentration of the Iodized Table Salt Samples.....	54
Table 7. Evaluation of the Developed Method to other Methods.....	56

List of Abbreviations

Abbreviation	Definition
%RSD	Percentage Relative Standard Deviation
ANOVA	Analysis of Variance
CMYK	Cyan Magenta Yellow and Key
CZE	Capillary Zone Electrophoresis
DESS	Deep Eutectic Solvent
DI	De-ionized
EF	Enrichment Factor
HBA	Hydrogen Bond Acceptor
HBD	Hydrogen Bond Donor
HSV	Hue Saturation and Lightness
IC-UV	Ion Chromatography with Ultraviolet Detection
ILs	Ionic Liquids
IOM	Institute of Medicine
LDR	Linear Dynamic Range
LLME	Liquid-Liquid Microextraction
LOD	Limit of Detection
LOQ	Limit of Quantitation
PC	Personal Computer
RDA	Recommended Daily Allowance
RGB	Red, Blue, Green
ROI	Region of Interest
SD	Standard Deviation

SDIC	Smartphone Digital Image Colorimetry
T3	Triiodothyronine
T4	Thyroxin
TRNC	Turkish Republic of Northern Cyprus
TSH	Thyroid Stimulating Hormone
UL	Upper Intake Level
UNICEF	United Nations International Children's Emergency Fund
URL	Uniform Resource Locator
UV-Vis	Ultraviolet Visible
WHO	World Health Organization

CHAPTER I

Introduction

The human body requires different nutrients for specific functions. Metabolism, eudemonia, and physiological improvement are functions that rely on the micronutrient iodine, which is primarily responsible for the development of the thyroid hormones, triiodothyronine (T3) and thyroxin (T4). A lack or shortage of iodine ultimately results in impairment in neural functions and body growth (Hassanien et al., 2003).

Iodine influences general metabolism and is essential for fetal and infant neurodevelopment as well as organ and tissue function. A healthy human body has 15-20 mg of iodine, with the thyroid gland accounting for 70-80%. Thyroid hormones are required for a wide range of physiological functions in almost all species, including physiological improvement, energy production, and organ growth, particularly in the brain. As a result, a shortage of iodine throughout crucial times of life can disrupt thyroid hormone formation, resulting in a metabolic slowdown and lasting brain impairment (Brough, 2021).

Nearly one-quarter of the world's population reside in regions with soil lacking in iodine, making it an official global concern. Women who show a shortage of iodine may give birth to children susceptible to attention deficit hyperactivity disorder (ADHD) (Azizi et al., 2003).

Even a minor iodine deficit can have a negative impact on a child's intellect and performance. Inherited low-iodine synthesis due to low hormone production by the thyroid gland is a dangerous disorder that affects neurological function permanently. Breastfed babies are fully reliant on the iodine content level in the lactating mothers' milk, making the babies more susceptible if the moms are lacking in iodine (Delange, 2001).

Excess iodine in the body, on the other hand, can cause hypothyroidism and hyperthyroidism. Another supplementary source of iodine is seafood, containing substantial levels, as reported by the iodine concentration study in drinking water and food (Dahl et al., 2004). It is however not quite sustainable as an iodine intake source, especially for women that are pregnant as the level of iodine is not sufficient for daily demand (Hatch-McChesney & Lieberman, 2022).

The primary source of iodine intake for humans is iodized table salt, with eggs, cereals, vegetables, and milk serving as supplementary sources (Kulkarni et al., 2013). In the past, potassium iodide was used to iodize table salt, however, potassium iodate is now more routinely used to avoid iodine shortage (Mortazavi & Farmany, 2014).

Changes in salt fortification, storage, shipping, and cooking processes can all result in insufficient daily iodine intake, which necessitate the need for iodine level evaluation in both primary and secondary sources.

Benefits of Iodized Table Salts

Healthy Pregnancy Support

Functions such as brain and bone development in babies are aided by the proper consumption of iodized salt, which also helps in the prevention of significantly delayed physical and cognitive development of an unborn baby (Awuchi et al., 2020). This impairment can cause a child to lose speech and hearing, as well as affect his or her physical motions. Miscarriages and under-production of thyroid hormones in pregnant women can be avoided with a healthy iodine level. Thyroid issues can arise or worsen during pregnancy and are frequently alleviated by increasing iodine levels (Jiskra et al., 2014).

Healthy Heart Promotion and Hydration

Iodized salt aids in the production of hormones that regulate heart rhythm and blood pressure. It also aids in the burning of fat aggregation which may lead to heart complications (Cappuccio, 2013). The replacement of body fluids and electrolyte regulation is improved by adequate salt consumption, as the efficient operation of body systems and organs is dependent on this equilibrium.

Boost Thyroid Function

Iodine is required by the thyroid gland to boost the production of thyroid hormones such as T3 and T4. These hormones are essential for good health because they control blood pressure, body temperature, and heart rate (Obregon et al., 2005).

Thyroid hormones are also required for proper bone and brain development during pregnancy and infancy.

Toxins and Bacteria Removal and Prevention

Certain categories of metals are quite harmful to the human body, including lead and mercury, which with proper iodized salt intake are repelled as body pollutants (Sachdev, 2022). Through this process a healthy pH level is restored and sustained. Tiredness, headaches, and irregular digestive tract movements which can be induced by pathogenic bacteria can also be prevented with proper iodized salt intake (Awuchi et al., 2020).

Sources of Iodine and Salt Iodization

The ocean is the primary source of iodine in the environment. Elemental iodine in the water is volatilized and returned to the soil via rain. Iodine's geographic distribution has been influenced by glacial, flooding, and leaching into the soil (Niwattisaiwong et al., 2017). Because of slower iodine cycling, mountainous places (e.g., the Alps, Andes, and the Himalayas) and areas with frequent flooding generally have iodine-deficient soil (Fuge, 2013). Iodine is abundant in seafood because marine plants and animals concentrate iodine from seawater. Other foods' iodine level varies greatly depending on the source and any additives. Radiographic contrast, bread containing iodate dough conditioners, red food coloring (erythrosine), and medications such as amiodarone are less prevalent sources of iodine (Zimmermann, 2009).

Recommended intake of Iodine

When the supply is adequate, the thyroid takes 50-60 μg of iodine each day to maintain homeostasis and hormone production. A set of dietary intake levels is recommended by the WHO and national academy of medicine (USA), children 9 to 13 years old a minimum level of 120 μg , males and females 14 years and above 150 μg and for pregnant and lactating mothers, 220 μg and 290 μg respectively. People

18 years and over lacking in iodine due to medical conditions are recommended a dietary upper intake level of 1100 µg (Jooste & Strydom, 2010).

Iodine Deficiency

More than a quarter of the global populace is affected by iodine deficiency resulting in the shortage of a vital body nutrient. Such a lack has been investigated to be the prevalent basis of goiter, which affects an approximate number of 2.2 billion individuals globally; however, not all goiters are caused by a lack of iodine (Andersson et al., 2007). The severity of iodine deficiency determines the frequency and severity of IDD. Low-deficiency individuals are prone to thyroidal infections, spanning from enlarged thyroid glands to formulation of region-specific goiter (endemic) as a result of low soil iodine levels (World Health, 2007). Severe deficiency causes diminished sexual productiveness and brain damage in adults (Mathews et al., 2021). Cognitive and physiological growth disabilities are also possible in children and infants (Delange, 2001).

Impact of High Iodine Intake

It can be challenging to diagnose high iodine status as it is infrequent. But as a yardstick measurement, a urinary iodine concentration of more than 250 µg/L median implies the possibility of excess (World Health, 2013). Excessive iodine consumption can cause hyperthyroidism, autoimmune thyroid disease, and papillary thyroid carcinoma. High levels in healthy persons can limit thyroid hormone synthesis, leading to increased thyroid hormone stimulation, enlargement, and formation of diffuse goiters as a result of limited thyroid hormone synthesis. The development of nodular goiter on the other hand which is most prevalent in elderly people is a consequence of the acute increase and sudden change in iodine consumption, most commonly noted in severe iodine deficit populations (Zimmermann, 2009; Zimmermann et al., 2008).

Highlight of the Problem

Despite the multiple advantages offered by the available approaches for determining iodate in table salt, they necessitate complex instrumentation, extensive skill, and/or a high analytical cost.

Therefore, the development of an easy to-use, inexpensive, fast and simple procedure for adherence to the recommended daily intake level of iodine (90-250 μ g) stipulated by the WHO and for quality control, is critical.

Objective of the Study

The study aims at establishing a green approach directed at the extraction, enrichment, and detection of iodate present in table salt by combining Deep Eutectic Solvent-Liquid Liquid Micro-extraction (DES-LLME) as a micro-extraction technique and Smartphone Digital Image Colorimetry (SDIC) as a detection technique.

Research Questions and Hypothesis

Considering the problem stated, it is thus necessary to formulate an approach to address the problem, highlighting some research questions to form a pathway. These research questions are;

- Is it conceivable for microextraction techniques to replace traditional extraction techniques in the analysis of complicated matrices?
- Are there other qualitative or quantitative procedures that produce comparable results to advanced instrumental processes but at an inexpensive cost?
- For trace and ultra-trace determination how sensitive will the method be?
- Can there be an improvement in the developed method's selectivity and sensitivity using a specific wavelength as a light source?
- Will the described approached be efficient and robust in the detection of analytes in complicated matrices?

Significance of the Study

A green microextraction procedure (Deep eutectic solvent liquid-liquid microextraction) combined with a simple alternative detection technique (smartphone digital image colorimetry) and thus enhancing sensitivity and selectivity, can produce comparable results and performances to high-end complex instrumental methods at a reduced cost and with less dependence on electrical energy, thereby being incredibly advantageous to under-funded institutions, laboratories, and industries in emerging regions.

CHAPTER II

Literature Review

Theoretical Framework

Many analytical methods for detecting and monitoring iodine in salt, food, and human samples are currently available. The yardstick method for the quantitation of this analyte in table salt has been over the years fundamentally conducted by the traditional iodo metric titrimetric analysis, involving the reaction of iodate with iodide to liberate iodine in the presence of an acid, followed by a reaction with the oxyanion thiosulfate in the presence of starch as an indicator.

Other techniques include iodometric reaction in the presence of sodium acetate (Kulkarni et al., 2013), flow injection amperometry (Jakmunee & Grudpan, 2001), high-performance liquid chromatography with diode array detector (HPLC-DAD) (Gupta et al., 2011), ion chromatography with integrated amperometric detection (Gosh & Lal, 2010), and spectrophotometric determination with UV (Silva et al., 1998).

Deep Eutectic Solvents

The hunt for metal-free ionic liquids (ILs) became increasingly popular once the notion of green chemistry was introduced in the early 1990s. The development of ionic liquids by the combination of an organic cation with a wide range of anions such as BF₄, PF₆, and Cl as the most frequent through a great deal of effort resulted in them emerging as a promising sect of solvents (Seddon & Volkov., 2003).

The ability of ILs to change chemically their cationic capability in conjunction with an array of anions has provided scientists with a diverse range of ILs exhibiting characteristic properties such as melting point, density, and refractivity. ILs were designated as green solvents due to their low vapor pressure and high boiling point, which promotes recycling. However, the "green affiliation" of these specialized solvents was widely disputed in published literature. Many investigations have highlighted the hazardous toxicity and poor biodegradability of most ILs. High-purity ILs are also essential since contaminants, even in tiny levels, influence their physical properties (Earles et al., 2004; Hou et al., 2008).

Furthermore, the substantial amount of salt and large volume of solvent needed to thoroughly exchange the ions for IL formulation is not ecologically beneficial. Such disadvantages, coupled with how expensive these liquids are, stagnated their growth industrially, giving rise to the need and urgency for procedures that will enable their use sensibly (Romero et al., 2008).

The expensiveness and toxic nature of ILs were subsequently addressed by the emergence of a new sect of solvents, called Deep Eutectic Solvents (DESs), which are the result of the combination of two safe, biodegradable, and cheap constituent making a low-temperature mixture.

Since the discovery of DES as green alternatives and replacements for toxic solvents by Abbott et al. in 2003, they have heightened the interest of researchers in a broad range of applications, such as extractions. According to the report by Abbott *et al.*, DES was formed upon combining choline chloride with urea, giving a melting point of 12 degrees Celsius. The mixing of urea molecules with ions of chloride reduced the melting point significantly. DES was also figured to be produced from the mixing of carboxyl group acids with choline chloride (Abbott et al., 2004).

To make a low, melting point DES, two constituents with nontoxic properties and high melting points, hydrogen bond acceptor (HBA) and a hydrogen bond donor (HBD) are commonly employed. A key characteristic of these innovative solvents is their capacity to generate a wide range of nontoxic low melting point drop mixtures with varied physical as well as chemical properties by just altering one or both components (Pena-Pereira & Namiesnik., 2014).

The first set of DES produced were water-loving highlighting their capacity to form hydrogen bonds and were categorically used for the extraction of hydrophilic analytes from solids or hydrophobic samples, with notable applications of such hydrophilic DES including organic synthesis, biofuel processing, and catalysis. However, in 2015, the theory of hydrophobic DES, through the coupling of capric acid with different quaternary ammonium salts for extraction of hydrophobic analytes was established by Van Osch and his colleagues. Onwards, there has been a variety of hydrophobic DES proposed for analytical applications. The significant physicochemical features of DES, ranging from their tuneability to their

nonflammability have earned them widespread recognition in the analytical chemistry sphere (van Osch et al., 2015).

Synthesis Of DES

The formation of a DES is a straightforward process completed in one-step. Typically, no byproducts are created, and neither solvent nor final product refinement is needed. Except for a few combinations that demand higher temperatures, the majority of DES can be produced by mechanically combining HBD and HBA at temperatures 50-100 °C in the right molar ratio. (Zahrina & Mulia., 2017).

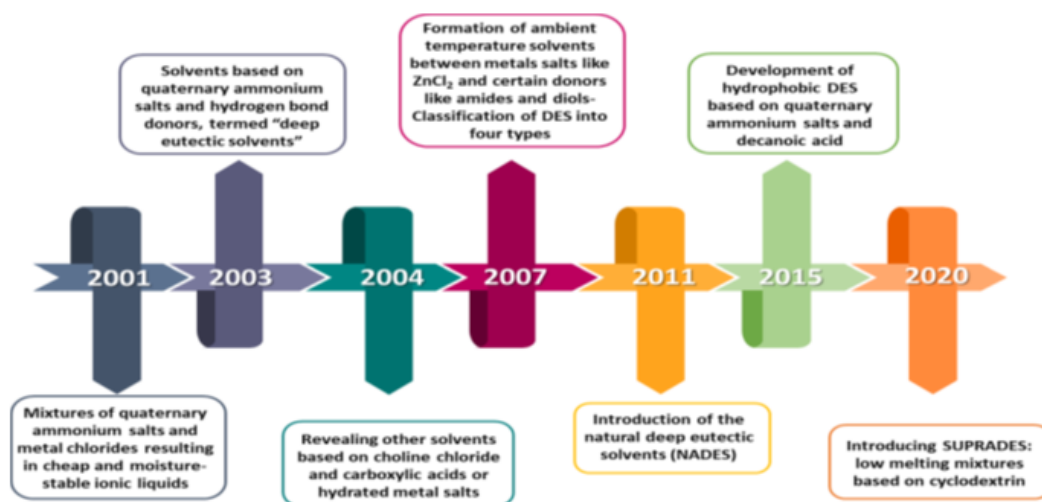
The constituents are combined, followed by heating of the combination until a clear, colorless, and consistent single-phase liquid is formed. This considerably reduces the cost of DES manufacturing compared to IL synthesis, which requires expensive starting materials and many purification stages. The purity of the raw starting ingredients generally controls the purity of the synthesized DES, thus making the reaction 100% in atom economy.

However, regardless of the preparation process, intense heat may potentially lead to the deterioration of the deep eutectic solvent (Rodriguez et al. 2019).

The grinding process involves combining the compounds at room temperature and crushing them with a pestle in a mortar until a clear liquid forms (Florindo et al. 2014).

Furthermore, because the precursors for these green solvents are widely reachable and affordable, DES may be produced on a large scale in industrial production (Russ & Koing, 2012). They have also been manufactured from aqueous solutions in some situations by grinding in a mortar, freezing drying or extruding (Gutierrez et al., 2009). Vacuum evaporation has also been proposed, which fundamentally involves the dissolution of the constituents in water followed by evaporation at a temperature of 50°C by using a rotary evaporator and drying by silica gel absorption.

Figure 1

The Evolution of DES Within the Last Decade

(Environmental Chemistry Letters (2021) 19:3397–3408)

Classes of DES

By mixing quaternary ammonium salts, an HBA, with metal salts at room temperature, molten salts were produced. Deep eutectic solvents are defined by the generalized formula Cat^+X_zY , where Cat^+ is any ammonium, phosphonium, or sulfonium cation in theory, and X is a Lewis base, typically a halide anion.

The complex anionic species are generated when X reacts with a Lewis or Bronsted acid Y (z denotes the number of Y molecules that interact with the anion). Classification of the deep eutectic solvent is dependent on the agent of complexation used. The first types and second types are utilized to produce water-loving DES, while the third and fourth types are utilized to produce water-repelling DES (Plastiras & Samanidou, 2022).

Table 1.

General Formula for the Formation of DES

Type	General Formula	Terms
I In ¹⁰	$\text{Ca}^+\text{X}^- = \text{MCl}_x$	$\text{M} = \text{Zn}^{1,5,6}, \text{Sn}^7, \text{Fe}, \text{Al}^8, \text{Ga}^9,$
II	$\text{Ca}^+\text{X}^- = \text{MCl}_x \cdot y\text{H}_2\text{O}$	$\text{M} = \text{Cr}^{11}, \text{Co}, \text{Cu}, \text{Ni}, \text{Fe}$
III	$\text{Ca}^+\text{X}^- = \text{RZ}$	$\text{Z} = \text{CONH}_2,^{12} \text{COOH},^{13} \text{OH}^{14}$
IV	$\text{MCl}_x + \text{RZ} = \text{MCl}_{x-1}^+ \cdot \text{RZ}$	$\text{M} = \text{Al}, \text{Zn}, \text{and } \text{Z} = \text{CONH}_2, \text{OH}$
	MCl_{x+1}	

American Chemical Society: (Chemical Review dx.doi.org/10.1021/cr300162p
Chem. Rev. 2014, 114, 11060–11082)

Physicochemical Properties of DES

Properties such as their physicochemical aspects are primary factors for the expanding attention in deep eutectic solvents. These green solvents can be chemically fine-tuned to meet certain requirements for specific applications aside from exhibiting thermal and chemical stability, nonflammability and reduced vapor pressure and volatility.

Listed below are the principal physicochemical features of DESs;

Freezing Point.

Because DESs are generated as the composition of two solids capable of producing a new phase, the resulting phase has a lower freezing point than the separate parts. For example, when ChCl and urea are mixed in a molar ratio of 1: 2, the freezing point of the eutectic is 12°C , which is significantly lower than the melting points of ChCl and urea (302°C and 133°C , respectively). The considerable decrease in freezing point is caused by an interaction between the halide anion and the hydrogen bond donor component, in this case, urea.

Recorded freezing temperatures of all DESs are less than 150°C. In general, DESs with freezing points lower than 50°C are more appealing since they can be employed as cheap and safe solvents in a variety of sectors.

Table 2.

Freezing Points of Some Common DES

Hydrogen bond donor (HBD)	ChCl: HBD (molar ratio)	T _m [*] /°C	T _f /°C
Urea	1: 2	134	12
Thiourea	1: 2	175	6
1-Methyl urea	1: 2	93	29
1,3-Dimethyl urea	1: 2	102	70
1,1-Dimethyl urea	1: 2	180	149
Acetamide	1: 2	80	51
Benzamide	1: 2	129	92
Ethylene glycol	1: 2	-12.9	-66
Glycerol	1: 2	17.8	-40
2,2,2-Trifluoroacetamide	1: 2.5	72	-45
Imidazole	3: 7	89	56

Royal Society of Chemistry: (Chem. Soc. Rev., 2012, 41, 7108–7146 7111)

Viscosity.

High viscosity is most usually associated with a DES, which importantly must be evaluated. Most deep eutectic solvents fall at a viscosity level greater than 100 centipoises (cP) at room surrounding temperature. The exception to this level of viscosity however is the green solvent mixture of choline chloride and ethylene glycol (EG).

The high viscosity characteristic of deep eutectic solvents is a result of the rich hydrogen bond interaction between the various constituents of the mixture, making the movement of free species within the solvent limited. Most DESs have

large ion sizes and relatively small void volumes, but additional factors like electrostatic or Van der Waals interactions may contribute to their high viscosity.

The development of DESs with low viscosities is preferable due to their potential applications as green media.

Table 3.

Viscosities of some common DES

Quaternary Salts	HBD	Salt : HBD molar ratio	Viscosities (cP)
ChCl	Urea	1 : 2	750 (25 °C)
ChCl	Urea	1 : 2	169 (40 °C)
ChCl	EG	1 : 2	36 (20 °C)
ChCl	EG	1 : 2	37 (25 °C)
ChCl	EG	1 : 3	19 (20 °C)
ChCl	EG	1 : 4	19 (20 °C)
ChCl	Glucose	1 : 1	34 400 (50 °C)
ChCl	Glycerol	1 : 2	376 (20 °C)
ChCl	Glycerol	1 : 2	259 (25 °C)
ChCl	Glycerol	1 : 3	450 (20 °C)
ChCl	Glycerol	1 : 4	503 (20 °C)
ChCl	1,4-Butanediol	1 : 3	140 (20 °C)
ChCl	1,4-Butanediol	1 : 4	88 (20 °C)
ChCl	CF ₃ CONH ₂	1 : 2	77 (40 °C)
ChCl	Imidazole	3 : 7	15 (70 °C)

Royal Society of Chemistry: (Chem. Soc. Rev., 2012, 41, 7108–7146)

Density.

A key physical attribute of any solvent and very essential in chemical reactions. Most documented deep eutectic solvents have densities greater than water, ranging between 1.0 and 1.3 g/cm³ at 25 °C, whereas metal salt-based deep eutectic solvents have densities in the 1.3-1.6 g/cm³ range (Tang & Row, 2013). Hydrophobic deep eutectics, on the other hand, have lower densities than water (Florindo et al.,

2019). The density of the deep eutectic solvent is temperature dependent, decreasing linearly with increasing temperature. Furthermore, the density is affected by the hydrogen bond donor and the molar ratio (Abbott et al., 2011).

Table 4.

Densities of some Common DES

Salts	HBD	Salt: HBD (mol : mol)	Density (ρ , g cm ⁻³)
EtNH ₃ Cl	CF ₃ CONH ₂	1: 1.5	1.273
EtNH ₃ Cl	Acetamide	1: 1.5	1.041
EtNH ₃ Cl	Urea	1 : 1.5	1.140
ChCl	CF ₃ CONH ₂	1 : 2	1.342
AcChCl	Urea	1 : 2	1.206
ChCl	Urea	1 : 2	1.25
ZnCl ₂	Urea	1 : 3.5	1.63
ZnCl ₂	Acetamide	1 : 4	1.36
ZnCl ₂	EG	1 : 4	1.45
ZnCl ₂	Hexanediol	1 : 3	1.38
ChCl	Glycerol	1 : 2	1.18
ChCl	Glycerol	1 : 3	1.20
ChCl	Glycerol	1 : 1	1.16
ChCl	Glycerol	1 : 3	1.20
ChCl	EG	1 : 2	1.12
ChCl	EG	1 : 3	1.12

Royal Society of Chemistry: (Chem. Soc. Rev., 2012, 41, 7108–7146)

Polarity.

Polarity is an important feature since it represents a solvent's total solvation capabilities. Despite its importance, the polarity of deep eutectic solvents has received little attention and has only lately been addressed. This property is frequently estimated using solvatochromic factors, which takes into consideration the hypsochromic or bathochromic shift of UV-vis bands as a function of solvent

polarity for negatively solvatochromic dyes (e.g., Reichardt's betaine dye) or positively solvatochromic dyes (e.g., Nile red) (Reichardt, 1994).

Deep Eutectic Solvents in Microextraction

DESs are useful for a wide range of macro and micro-scale applications, such as microextractions, due to their particular physicochemical properties. The intensity of hydrogen bonding between the two components, as well as the molar ratio, all influence the level of melting point drop. An effective extraction agent can be a liquid DES generated at ambient temperature.

An important aspect for consideration in the utilization of a DES as a potential extraction solvent is its density. It is quite easier to collect a DES that is heavier than water from an aqueous sample solution after extraction (Jia et al., 2020). In microextractions, low-density DES, having freezing and melting points near that of ambient temperature, can be collected by solidification of the extracting agent's floating droplets (Zeng et al., 2017).

In order to obtain an extraction balance in microextractions, low-to moderate viscosity solvents are rapidly disseminated by mechanical agitation (Yilmaz & Soylak, 2020).

Deep Eutectic Solvent as Extraction Solvent in Liquid-Liquid Microextraction

Because of benefits such as simple operation, fast extraction time, high enrichment factor, and inexpensive analytical costs, liquid-liquid microextraction (LLME) has received a lot of attention. More importantly, a faster extraction and shorter analytical time are achieved with LLME employed in batch mode completing extraction quickly. The use of halogenated solvents, which are denser than water, for extraction is a significant disadvantage of many current LLME methods. These solvents are potentially hazardous to both the environment and the analysts due to their toxicity and volatility. The evolution of "green extraction agents," which meet the specifications for an extraction agent in traditional LLME processes while also significantly reducing the volatility and toxicity of the extraction agent (thus

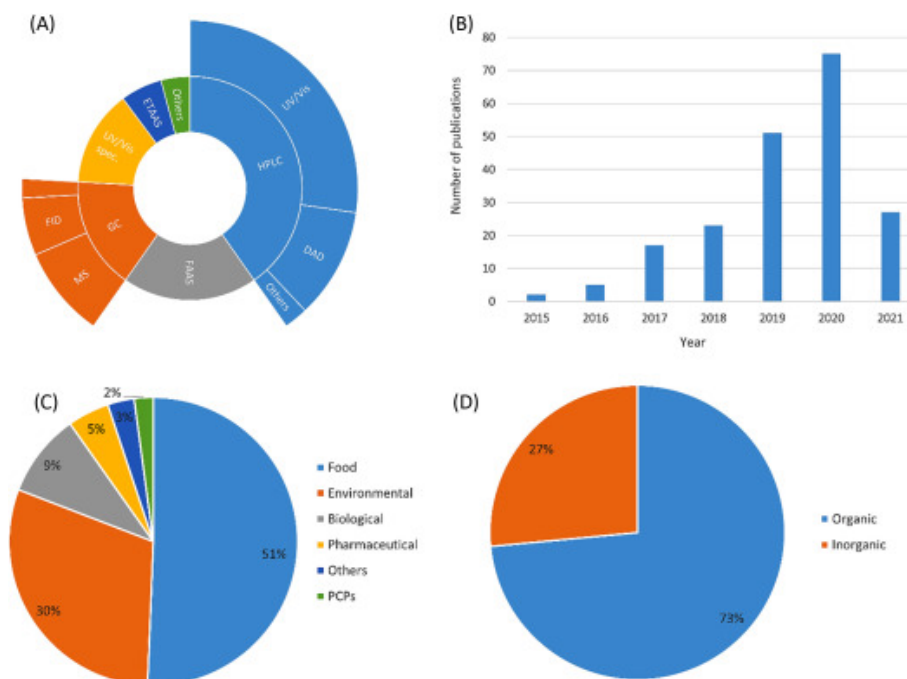
reducing the risks to operators), has thus piqued the interest of researchers (Zhu et al., 2018).

The employment of DES in liquid-liquid microextraction has seen a significant expansion of the volume of applications with respect to analytical chemistry for the identification of a broad range of analytes constituting a variety of samples ever since its introduction in 2015 by Dadfarnia. Conclusion of that study suggested that a 1:1 molar ratio of $\text{ChCl}:\text{Urea}$ is an inexpensive, safe solvent for the ligand-free targeting and enrichment of lead and cadmium in culinary oils before spectroscopic detection (Karimi et al., 2015).

Following this discovery, procedures for the extraction of both inorganic and organic analytes by liquid-liquid microextraction methods coupled with deep eutectic solvent were established, improved, then integrated with a wide range of analytical approaches for analyte identification. Illustrated by the expanding collection of literature on liquid-liquid microextraction technique based on deep eutectic solvents, the usefulness of these green solvents in microextraction is highlighted. A large variety of samples, including food and environmental samples demonstrates the method's efficacy.

For complicated matrices, sample cleansing is an essential step before LLME. Deep eutectic solvent-based liquid-liquid microextraction can be used directly on simpler samples, such as water, without or with limited sample processing, such as filtering and/or dilution. Prior to DES-LLME, more thorough sample cleansing methods for complex matrices were developed.

Figure 2

Applications of the Green Solvent (DES) in Liquid-Liquid Microextraction

A) the different types of instruments used, (B) volume of DES-LLME publications, (C) extracted sample types with DES-based LLME, (D) different type of analytes determined after the application of DES-based LLME. (Secondary data from “deep eutectic solvent in microextraction”; Alshana & Soylak., 2021)

Digital Image Colorimetry on a Smartphone

The explanation and quantitation of the human sense of sight is scientifically called colorimetry, and is generally separated into two classes; an optical form referred to as visual colorimetry, and an optoelectrical form called photoelectric colorimetry (Fan et al., 2021). The first uses the naked eye to detect concentration through observation of color changes, but the latter uses measuring systems like a spectroscopy, being additionally selective and efficient in measurement which is more efficient in selectivity and quantitation (Clydesdale, 1978). Due to this, colorimetric quantitation is being extensively done by photoelectric colorimetry. The subdivision of colorimetry that digitalizes images taken by digital cameras,

smartphones and webcams is referred to as digital image colorimetry (Firdaus et al., 2014).

DIC has gained tremendous momentum in recent years as a result of mankind's urgency in the capturing, then distribution of information in real-time. The most extensively used picture-capturing tools in this regard are smartphones and digital cameras, due to their obvious mobility, lightweight, and advancement in camera systems and applications (Coskun et al., 2013). The utilization of the camera on a smartphone as capturing device for a digital image colorimetric system will form the basis for subsequent discussions. As a result, smartphone-based digital image colorimetry will be referred to as SDIC.

There are two primary steps involved in SDIC:

- Capture of image by smartphone
- Measurement of captured image using a processing tool such as ImageJ or adobe photoshop.

An appropriate colorimetric box is required to be built for this approach to ensure the capture of consistent images free from daytime interferences, while being considerate of the essential elements of an optical instrumentation.

Instruments that function in the ultraviolet-visible, visible, and IR region of the electromagnetic spectrum are referred to as optical instruments. The visible part of the spectrum is used by SDIC since the human eyes operate in that region. The development of the colorimetric box, serving as the detection unit of the system, is based on the primary elements of an optical system.

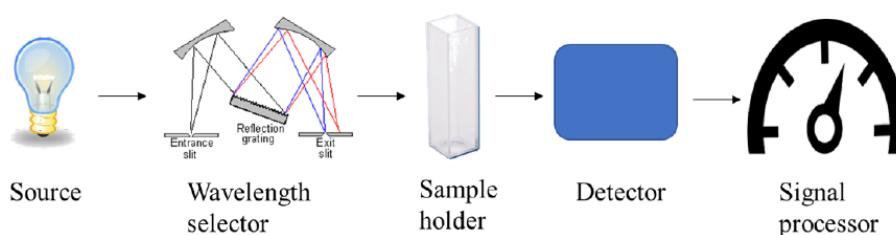
With all optical instruments, the fundamental components are identical but with varying configurations depending on their operation specific to an area of the electromagnetic spectrum (Figure 3) (Skoog et al., 2017).

An optical instrument's basic components are as follows:

- A steady light source that emits radiant power.
- A transparent sample container.

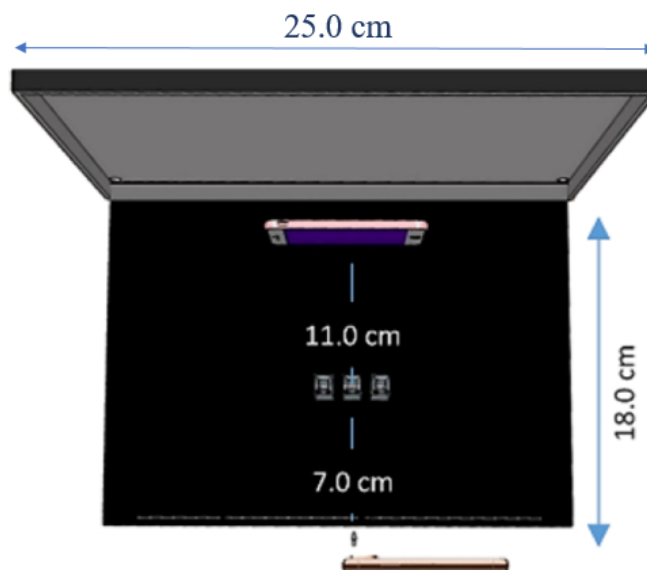
- A wavelength selector for picking out a certain portion in the electric or magnetic radiation range for quantitation.
- A detection system that transforms light energy into an electrical communication to be used.
- A signal converter that depicts the data as a scale.

Figure 3

Configuration of an Optic System*Assembling of the Colorimetric Detection System*

The detection box was designed to look like a fundamental optical equipment, made from aluminum with dimensions 25 X 18 X 9 cm in length. For this study, the interior of the in-house built colorimetric box is black, with a smartphone display serving the single-line light source combined as a wavelength generator, releasing a distinct path of electromagnetic energy. The other component of the system includes the sample holder capable of allowing the transmission of light, a smartphone for image detection and the signal converter which is an open-sourced ImageJ software.

Figure 4
Colorimetric Box



Optimized Parameters of the SDIC System

To ensure greater performance from SDIC, it is necessary to adjust certain crucial factors, such as;

- Wavelength of the single-line light source.
- Designating the preferred RGB channel.
- Optimal distance between detection camera and sample solution.
- The specified area for measurement (ROI).

Wavelength of the Single Line (Monochromatic) Light Source.

Spectroscopic systems used in the ultraviolet and visible region of the electric and magnetic range are characterized by higher absorbance range specific to a variety of analytes, illustrating the importance associated with the monochromatic wavelength of the light source. Analytes, being specific only to certain wavelengths of the electromagnetic spectrum are characterized by the vivid response of a particular color identified upon adjustment of the RGB model. To achieve this

optimum response, adjustment of the single-line light source in the RGB color space is done by utilizing a program that can convert a wavelength to its respective color. For example, wolfram is a free online converter capable of performing the task of converting a selected wavelength under the visible region to its corresponding color. After generating the required color from the online converter, Microsoft paint is utilized to attribute proper dimensions to it, then transferred via cloud storage or means to the device selected for the backdrop display. It is paramount to evaluate the response of a variety of wavelengths corresponding to the associated colors of an analyte and the wavelength with the strongest signal selected.

Preferred Red, Green, and Blue Channel.

To harmonize and regulate colorimetric quantitation, color spaces such as the hue-saturation-value model (HSV), the cyan-magenta-yellow-black model (CMYK) and the red-green-blue model (RGB) were developed (Capitan-Vallvey et al., 2015). A numerical value, corresponding to the pixel strength of the color model gives analytical information. This RGB color model, engineered for computer-enabled display devices, is expressed as a cubic shape in a three-dimensional orientation, assigning a particular color to one specific apex of the three rectangular axis points. An element from each of the RGB points contributes, in varying degrees, to the color tube.

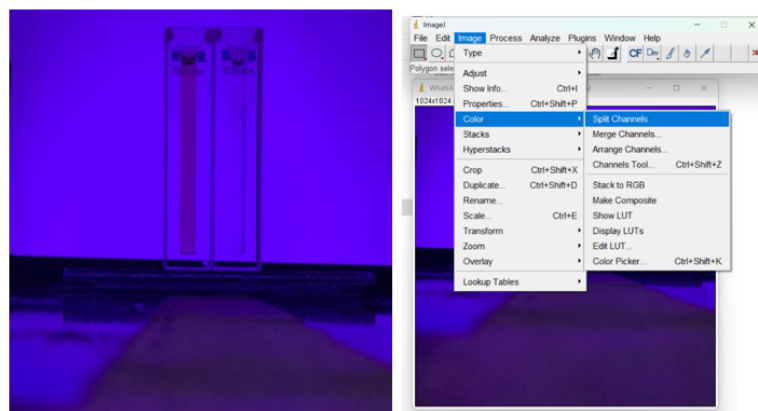
For each of the points on the tube, three numbers are associated corresponding as triplicates of the Red, Blue, and Green channels, spanning from a complete black to a complete white, depicted as (0,0,0) and (255, 255, 255), ultimately creating a number for each channel (Fan et al., 2021). Of the different channels of this model, a particular channel delivers an optimal signal specific for a particular analyte, in contrast to the other channels and identified by means of a unique coloration. A split of the captured image into the respective RGB channels is quite mandatory to enable the respective selection of the optimum channel. This process can be achieved using an applicable software program designed to convert image signals to numerical data, such as the ImageJ software, from which the selection of 'file' from the user interface followed by 'open' is inputted as commands to navigate the directory in which the acquired image is stored. From the drop-down menu, choose 'image,' then 'color,' and finally 'split channels.' Three RGB channels

will be created in the image. The most intense channel can be chosen for analysis. In this picture, the B channel is the most vivid.

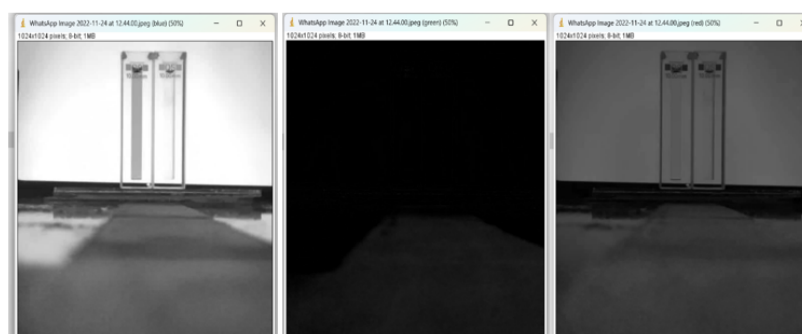
Figure 5

Selection of RGB Channel

(a)



(b)



Optimal distance Between Detection Camera and Sample Solution.

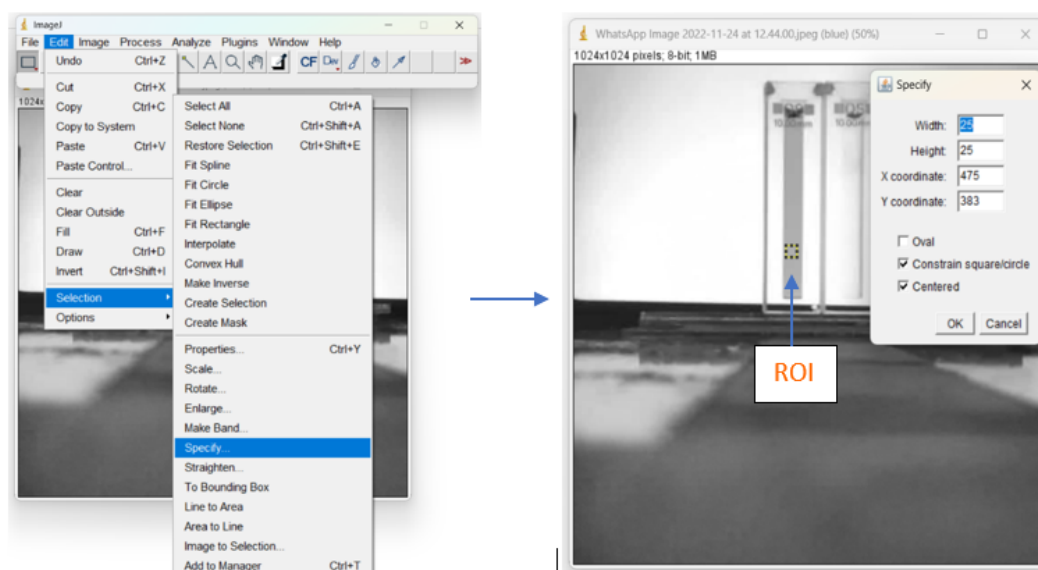
Optimizing the length between the sample solution and analyte is necessary because too near or short a distance gives blurry images, resulting in over pixelation, which in turn produces images that are unfit for data processing, as they are far from being a true representative of the sample solution. This is overcome by ensuring that the focus of the capturing camera is at a distance that will give clear and vivid reproducible replicate images for quantitation. Provided other factors, including camera lens, dimensions and autofocus configurations are kept unchanged, the efficiency of the detection device is optimal (Zhang et al., 2018).

Specified Area for Measurement (ROI).

The highlighted region designated by the program to transform the pixel strength into a value that may be connected to the concentration of the analyte for quantification is known as the region of interest (ROI). To select the ROI, go to 'edit.' In the dropdown menu, select 'specify' and then 'selection.' A drop-down option is displayed, which allows the user to select the form and alignment of the ROI. A square, centrally placed is selected for this study. The sample solution's X and Y coordinates should be modified, and the ROI's width and height should be written. The chosen figure which will be equal to px^2 represents the ROI. For further analysis, $\text{ctrl} + \text{shift} + \text{E}$ can be employed as a short code to insert the ROI along with the desired characteristics. This immediately displays the ROI.

Figure 6

Highlighting the Region of Interest



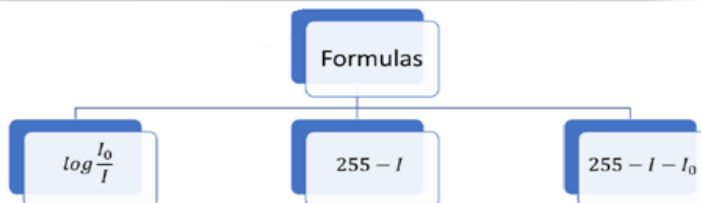
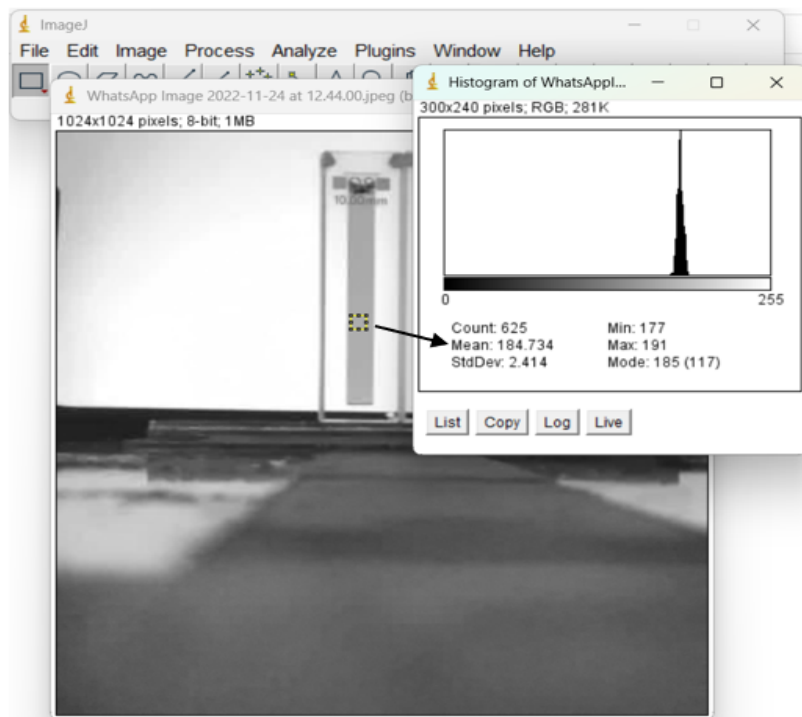
Signal Conversion.

The response of both the blank solution and the sample solution are each represented by a histogram depicted by the symbols I_0 and I respectively in a specific channel and given a numerical value. Signifying a perfect blank, 255 is the number

generally utilized, starting from 0. The numerical value of the histogram, given as the response of both I_0 and I , gives information on the concentration of the analyte.

Figure 7

Signal Conversion



Converting Signal into Concentration.

A histogram can be generated from the ROI of the highest intensity channel by clicking on the 'Analyze' menu followed by the 'Histogram' menu (or Ctrl H), from the drop-down option of the software. The mean value of the histogram is used for quantification. SDIC, on the other hand, has an inverse connection with analyte concentration, as opposed to certain optical systems wherein the signal is directly

proportionate to it. Because of this, a rise in the intensity of the color depicts an increase in analyte concentration as the mean value of the histogram lowers.

Therefore, be it absorbance or reflectance that is evaluated, various equations to generate a positive linear relationship in the calibration plots for measurements have been formulated. The most often used formulas are depicted in Figure 7. (Porto et al., 2019).

The Analyte

Iodate

A significant lack of iodine in the body can result in iodine deficiency disorders which includes infant mortality, goiter, infertility, dwarfism, and miscarriage (Eckhoff & Maage, 1997). Detrimental health repercussions such as hyperthyroidism can occur in the body as a result of overabundance of iodine (Leung & Braverman, 2014). With such grave concerns, The WHO recommends a daily iodine intake of 90 μg for children and 250 μg for pregnant women (Chandra et al., 2019). The primary source of iodine intake for humans is iodized table salt, with eggs, cereals, milk as supplementary intake (Kulkarni et al., 2013).

Preventing the impairment of body functions and intellectual disability as a result of iodine deprivation, has been a global effort. Primarily spearheaded by the WHO and national academy of medicine, with stipulations and recommended daily intake levels for iodine, potassium iodate is now used for the iodization of table salt (Mortazavi & Farmany, 2014). The quantitation of this analyte in table salt has been over the years fundamentally conducted by the traditional iodo metric titrimetric analysis, involving the reaction of iodate with iodide to liberate iodine in the presence of an acid, followed by a reaction with the oxyanion thiosulfate in the presence starch of as an indicator.

Several different techniques have been proposed for iodate in table salt quantitation such as iodo metric reaction in the presence of sodium acetate reported by (Kulkarni et al., 2013), flow injection amperometry (Jakmunee & Grudpan, 2001) and ion chromatography with integrated amperometric detection (Gosh & Lal, 2010).

CHAPTER III

Materials and Methods

Consumables

The chemicals together with all reagents utilized for the research and investigation of this thesis were of analytical grade, unless otherwise noted. Phenol (Ph) and Potassium Iodide (KI) were acquired from Riedel-de Haen (Germany). Sigma-Aldrich (Germany) supplied Choline Chloride (ChCl), Ethanol (EtOH), and hydrochloric acid (HCl). Potassium iodate standard was procured from Merck (USA).

Apparatus

For this investigation, reproducible images were captured using a 5th generation iPad mini embedded with a back camera of 8 MP with a f/2.4 aperture. The permanent memory capacity is 65GB, 3GB RAM, coupled with an Apple A12 Bionic chip processor. A touch display screen of 1536 by 2048 pixels resolution and measuring 7.40 inches diagonally.

As means of the single line radiation source a second smartphone (iPhone 12 pro max), with a 6.7" touch screen display, 1284 X 2778-pixels resolution, coupled with a 12 mega pixel camera, 128GB storage, an A14 Bionic chip with a 6GB RAM on a 2X3.1 GHz firestone processor was employed.

The colorimetric box was designed to look like a fundamental optical equipment, made from aluminum with dimensions 25 X 18 X 9 cm in length. For this study, the interior of the in-house built colorimetric box is black to enable an illuminance-free environment with a hole approximate in size drilled into the box's side to allow image capture of the sample solution by the camera. The system was fine-tuned to meet the requirements of optimized parameters as described in chapter 2.

A Purelab Ultra Analytic De-ionizer (UK) was employed to produce deionized (DI) water, which was then utilized to produce all aqueous solutions.

Conversion of an acquired image into analytical data was carried out by use of the ImageJ processing software.

Calculation of $\log P$ and pK_a values was done using MarvinSketch by ChemAxon Ltd.

Vortexing of all samples was done using a digital vortex MS3 by IKA Germany. All sonication process was done using an ultrasonic bath from Isolab Germany and centrifugation of samples was carried out using a portable EBA20 centrifuge from Hettich Germany. Eppendorf micropipettes were used for the measurement and transfer of precise volumes of sample solutions and solvents. Standards and samples were weighed with an electronic balance (Mettler-Toledo, Switzerland).

Using a single beam UV-visible spectrophotometer (PG Instruments, UK) at a wavelength of 400 nm, separate experiments were conducted to determine the method's efficiency.

Statistical Analysis

Single-factor analysis of variance (ANOVA) was performed using Microsoft excel 365 for windows to statistically evaluate the performance of the proposed system.

Sample Preparation

Samples of table salt (labeled T1 through T5) were bought at community stores in Famagusta, TRNC. They were then kept in a dry, dark environment until usage. For experimental analysis, 2.0 g of the sample was accurately measured into a volumetric flask (25.0 mL), and sufficient DI water was added to sonicate for 5.0 minutes at a temperature of 25°C/KHz in order to completely dissolve the salt, and then filled with additional DI water to the volume mark.

Preparation of Solutions

Stock Solution

A stock solution of 50 mmol L⁻¹ of IO₃⁻ was prepared from KIO₃ (1.07g). An intermediate solution of 1.0 mmol L⁻¹ was prepared with DI water in 100 mL volumetric flask. From this intermediate stock, working solutions ranging from 50 to 250 μmol L⁻¹ and 10 to 50 μmol L⁻¹ concentrations were prepared for SDIC and DES-LLME, UV/Vis calibrations respectively.

Potassium Iodide Solution

10 g of solid KI was dissolved in a pre-boiled and cooled DI water in a 100 mL volumetric flask. The DI water was boiled and allowed to cool to room temperature because normal DI water contains dissolved oxygen that can react with the I⁻ and oxidize it to I₂, which will turn the solution yellow.

Preparation of 1.0M HCl Solution

8.33 mL of concentrated Hydrochloric acid (HCl) was transferred by pipette to a 100 mL volumetric flask and diluted with DI water to the mark.

Preparation of Salt Sample Solution

A 10.0 g of salt was dissolved in 50.0 mL volumetric flask and used as the sample solution.

Redox Reaction for Iodate Quantitation in Table Salt

The traditional redox titration is the primary procedure for the measurement of IO₃⁻ in iodized salt. The reaction is as follows;

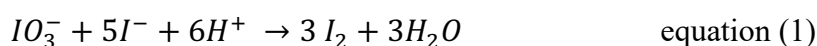
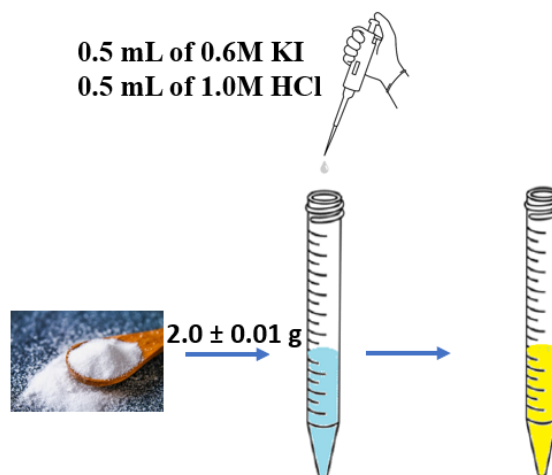


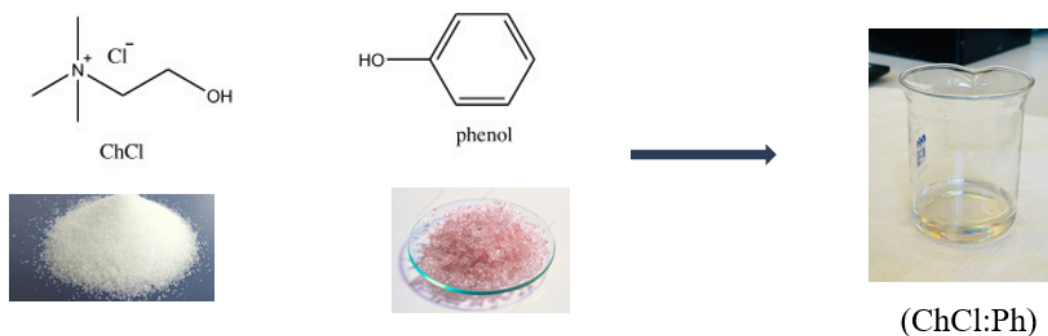
Figure 8

Simplified Diagram of the Redox Reaction**Synthesis of the Deep Eutectic Solvent (DES)**

DESs are useful for a wide range of large and small-scale applications, including micro extractions, due to their particular physicochemical properties. The intensity of hydrogen bonding between the two constituents, as well as the molar ratio, all influence the level of melting point drop. An excellent extraction solvent can be a liquid DES produced at ambient temperature.

As a result, Choline Chloride and Phenol (ChCl: Ph) was selected as the choice of green solvent due to its relatively simple synthesis at room temperature, its ability to mix and separate from other solvents due to its miscibility gap and density, making it a very effective and efficient micro extraction solvent.

Figure 9

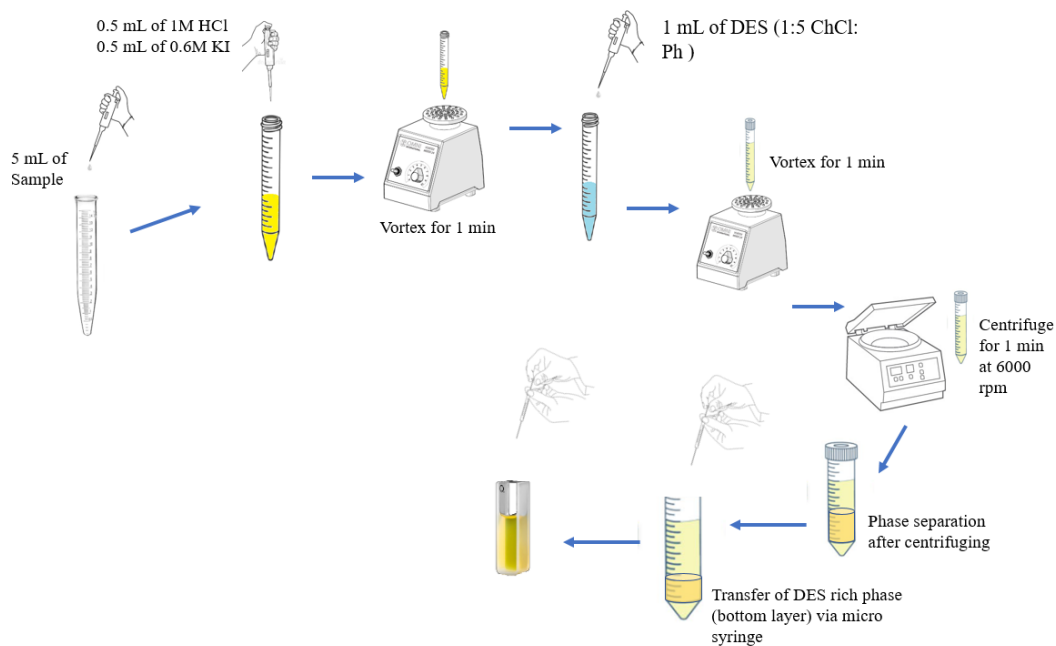
Synthesis of the Deep Eutectic Solvent**Reaction Procedure**

Into a screw-on 15 mL graduated centrifuge tube, 5 mL of the prepared sample solution was dispensed.

0.5 mL of 1.0 M HCl and 0.5 mL of 0.6 M KI were then added to this solution turning it yellow indicating the formation of I_2 .

The solution was vortexed for 1.0 min, and 1.0 ml of 1:5 ChCl: Ph (DES) was added forming very briefly a cloudy solution which was then mechanically agitated by vortexing for 1 min and centrifuged at 60 x 100 rpm for 1 min resulting in the formation of diphasic solution, with the analyte rich DES at the bottom.

Figure 10

Schematic Diagram of DESLLME**Signal Conversion**

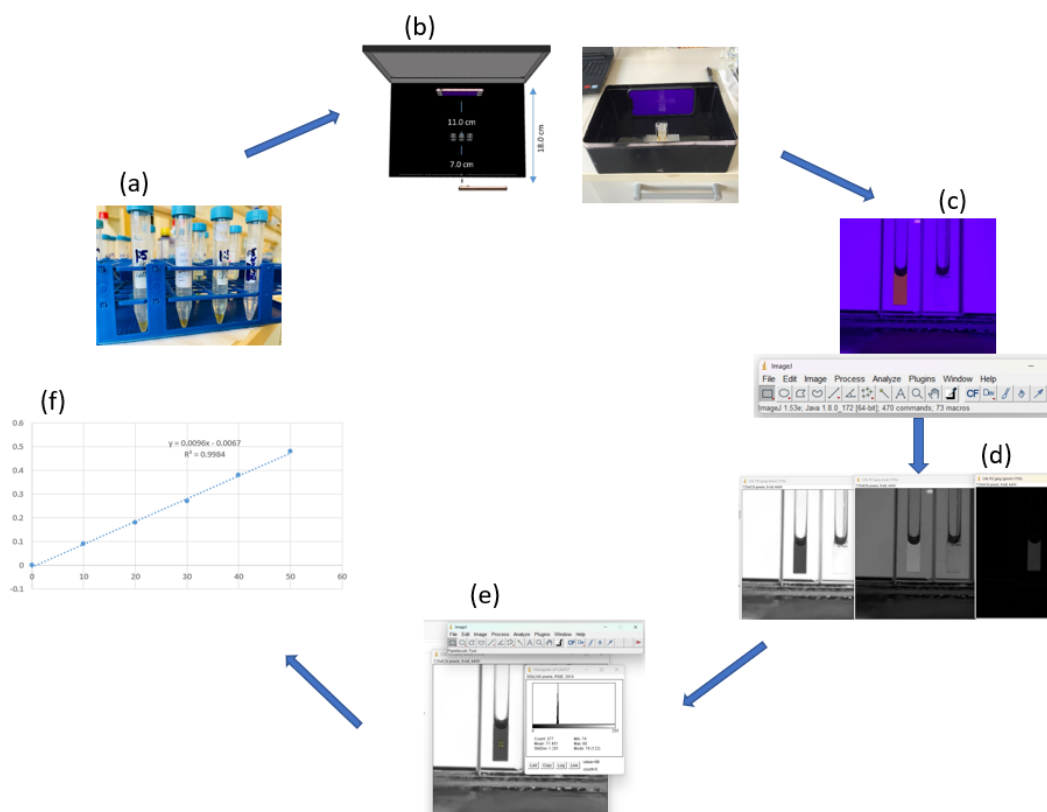
Upon the capture of the required images, they were subsequently sent through airdrop to the personal computer for ImageJ processing. They were split into their respective red, green, and blue channels with the blue channel providing the best response and thus selected for all analysis.

The formula

$$R = I_0 - I_S \quad \text{equation (2)}$$

where I_0 and I_S are the mean intensity of the blank and sample solution respectively, obtained from the blue channel's histogram, to calculate the response R .

Figure 11

Proposed SDIC System

- (a) Sample solution spiked with incremental concentrations of iodate standard;
 (b) The in-house detection system; (c) Extracted and preconcentrated analyte solution; (d) Red, Green, Blue channels of the split sample image; (e) Regression graph of calibration.

CHAPTER IV

Results and Discussion

Determination of Iodate in Table Salt by Deep Eutectic Solvent Liquid-Liquid Micro-Extraction Prior to Smartphone Digital Image Colorimetry

Optimization of The Deep Eutectic Solvent Conditions

Molar Ratio of the DES.

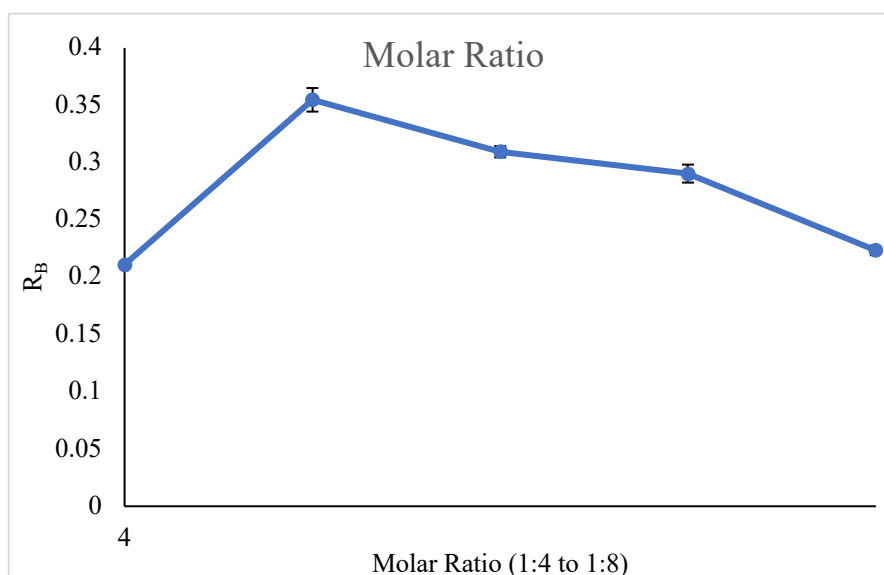
The effect of HBD to HBA molar ratio composition of the deep eutectic solvent in the microextraction procedure was investigated.

Molar Ratio of 1:4 to 1:8 ChCl: Ph were studied, with 1:1 to 1:5 having previously studied in a preliminary experiment.

The molar ratio of 1:5 ChCl: Ph gave the optimum response studied in the micro-extraction procedure and was used for all analyses.

Figure 12

Selection of the DES Molar Ratio



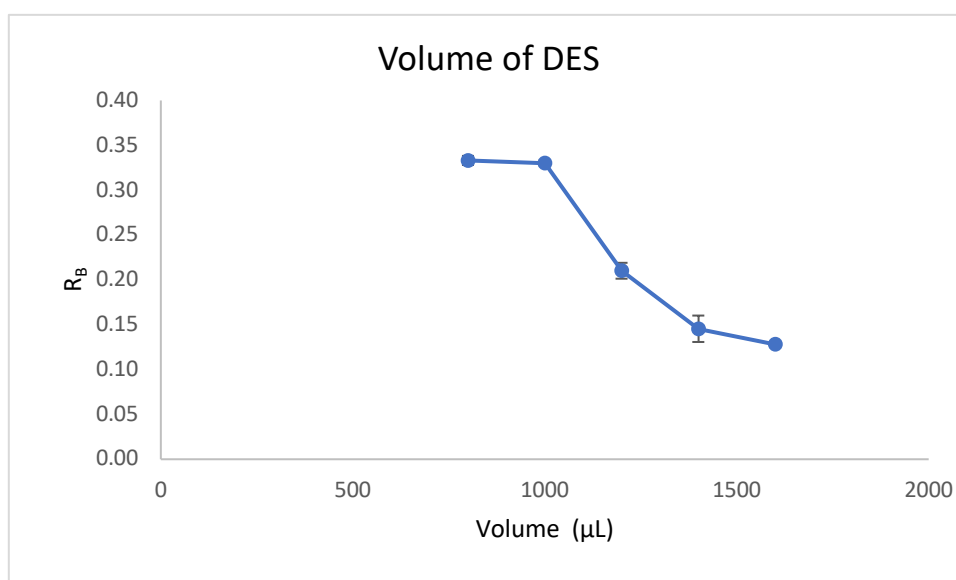
Volume of the DES.

The volume of the optimum molar ratio of the DES (1:5) was evaluated by studying varying sizes from 800 to 1600 μL .

An optimum response was observed from 800 1000 μL after which there was a downward trend. A Volume of 1000 μL DES yielded an optimum signal and was selected for all analyses as it demonstrated sufficient volume for miscibility and preconcentration.

Figure 13

Selection of Volume of DES



Emulsifying Agent.

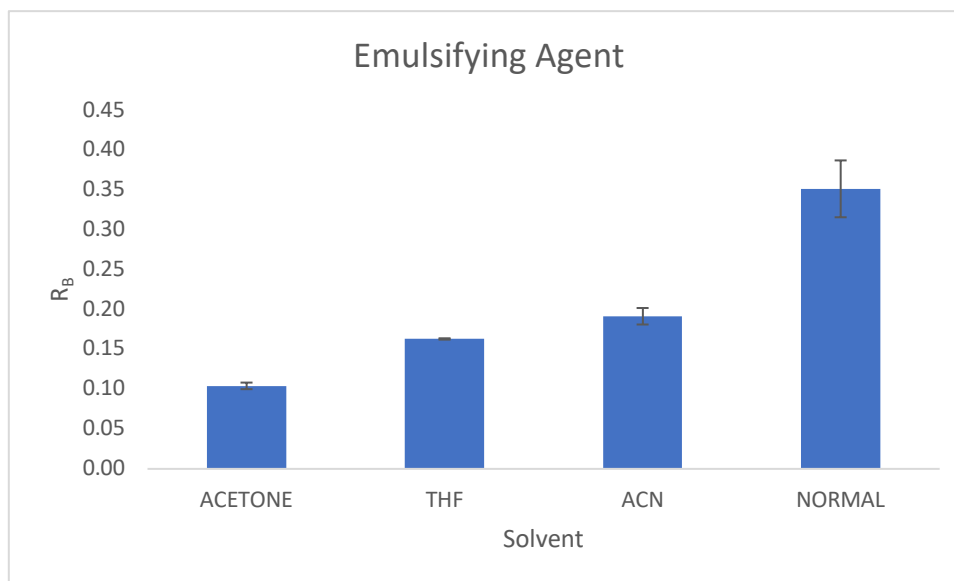
In an effort to enhance the miscibility of the DES with the sample solution, three different emulsifiers were studied (Acetonitrile, Acetone, and Ethanol) along with a sample containing no emulsifier.

The sample without any emulsifier gave the optimum response, indicating that the DES in its optimal volume and molar ratio was suitable enough to mix with the sample solution thoroughly and separate upon centrifugation forming a rich DES-analyte bottom layer.

Therefore, no emulsifying solvent was used in the proposed method.

Figure 14

Study of the use of emulsifying solvent



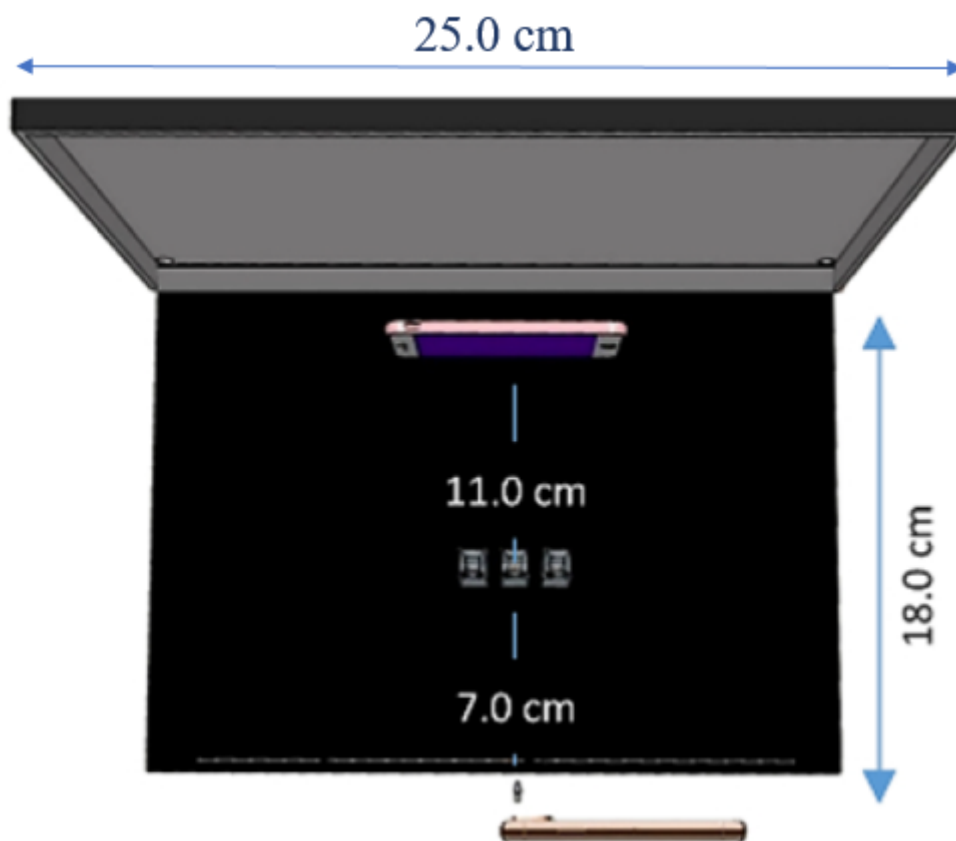
Optimization of Parameters of the SDIC System

Construction of the Detection Box.

A colorimetric box was designed to look like a fundamental optical equipment, made from aluminum with dimensions 25 X 18 X 9 cm in length. For this study, the interior of the in-house built colorimetric box is black to enable an illuminance-free environment with a hole approximate in size drilled into the box's side to allow image capture of the sample solution by the camera, which is 8 cm away from the quartz sample solution container. To avoid oversaturation of the lens of the camera, the intensity of the monochromatic light source was kept at a constant level and the backdrop was centrally placed.

The sample was then photographed using the back camera with the flare switched out.

Figure 15

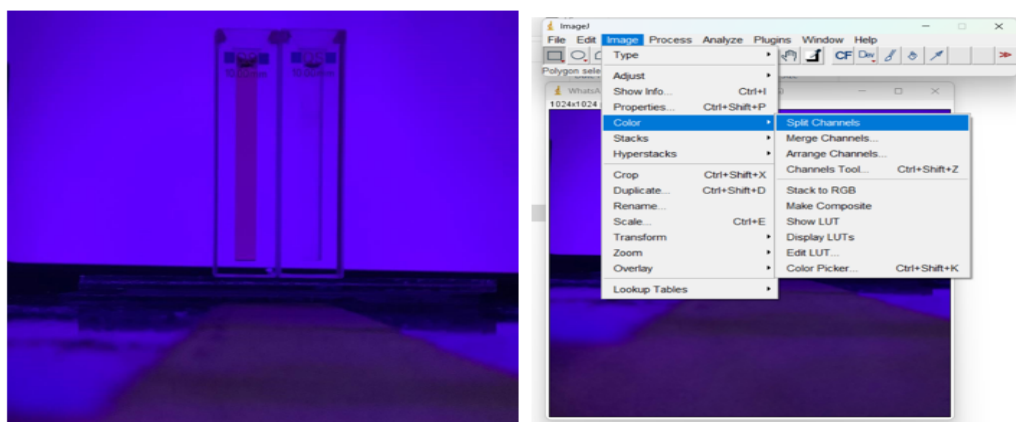
Schematic Diagram of the Colorimetric System**Selection of the RGB Channel.**

As illustrated earlier, a particular channel is specific to the sample solution upon splitting the captured image using ImageJ software. This channel, characterized by the low value of the mean of the histogram is selected as the optimum channel for analysis. For this study, the blue channel gave optimum results.

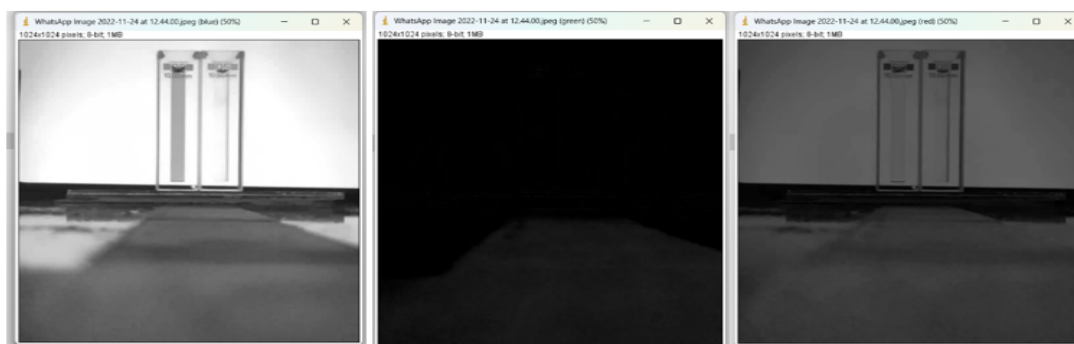
Figure 16

RGB Channel Selection

(a)

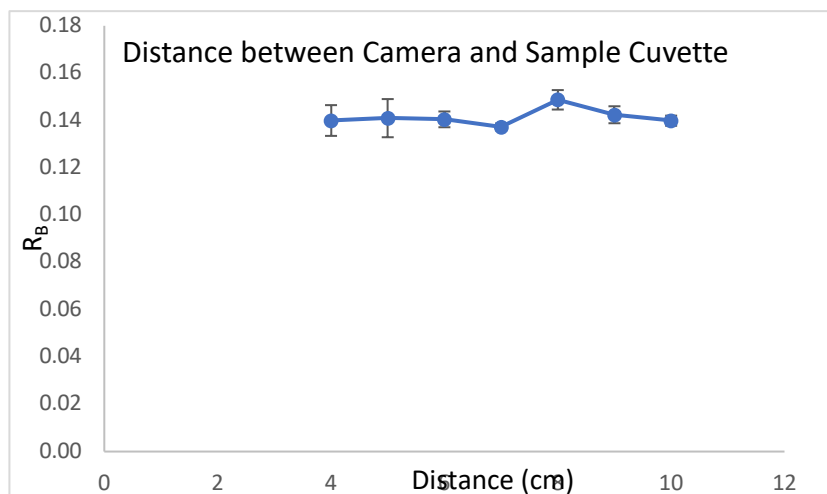


(b)

**Optimal Length Between Detection Camera and Sample Solution.**

The possible influence of the range between the capturing camera and the sample cell was investigated by measuring a range between 5.0 and 12.0 cm. At a distance of 5 centimeters, the camera's focusing was weak, culminating in a grainy, fuzzy image of the sample cuvette. A clarity in image occurred at a distance of 8cm between the camera and the cuvette, with sharper images observed from 9.0 cm to 12.0 cm. A decision was made on the distance of 8.0 cm giving the optimum response to compromise between sensitivity and repeatability.

Figure 17

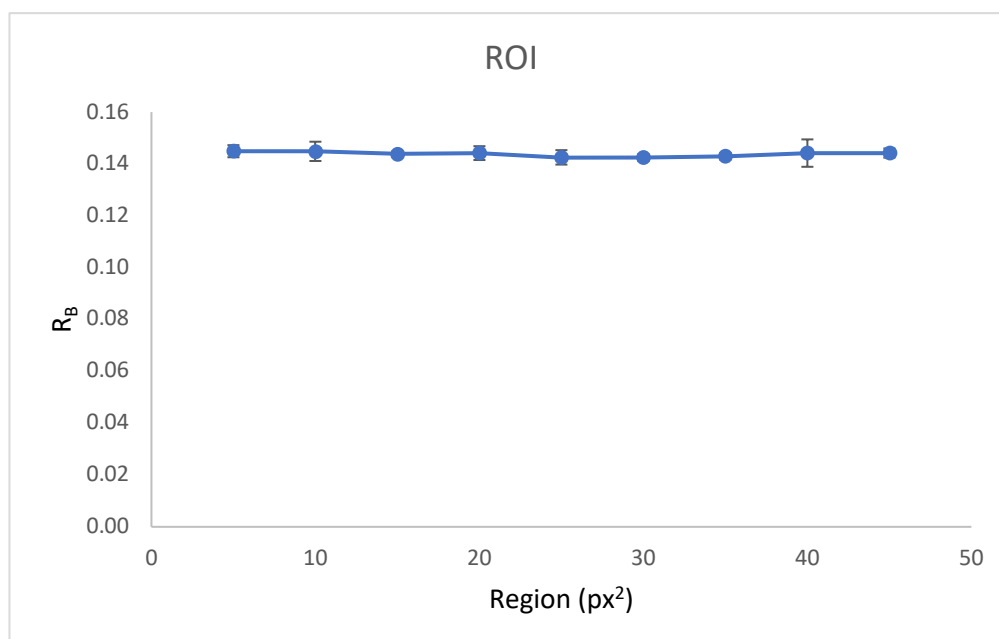
Optimal Distance Between Detection Camera and Sample Solution**Specified Area of Measurement (ROI).**

The highlighted region designated by the program to transform the pixel strength into a value that may be connected to the concentration of the analyte for quantification is known as the region of interest (ROI).

The sample solution's X and Y coordinates should be modified, and the ROI's width and height should be written. The chosen figure which will be equal to px^2 represents the ROI. The ROI was analyzed by altering the targeted area between 5 to 45 px^2 .

The working sample being homogeneous, there was no effect from any ROI, as indicated by the consistent response. Consequently, any ROI may be selected for measurement. 25 px^2 was determined to be the optimal ROI.

Figure 18
Specified Region of Interest (ROI)



Analytical Performance of the Deep Eutectic Solvent Liquid-Liquid Micro-extraction

Using the iodate standard in concentrations ranging from 10 to 50 μmolL^{-1} and 50 to 250 and 300 μmolL^{-1} , matrix-match calibration graphs were plotted using SDIC only, DES-LLME-SDIC and UV-vis spectrophotometric procedure to assess the proposed method's analytical performance. All methods showed good precision as demonstrated by their respective calculated intra-day and inter-day values.

Prior to DES-LLME-SDIC using the pure salt sample (NaCl), quantitation of the salt samples using the redox reaction only with SDIC was carried out, giving relative absorbances ranging from 0.06 to 0.13.

A summary of the collected data, demonstrating adequate performance as indicated by satisfactory proportionality (linearity) and adequately fitted coefficients of determination R^2 0.9951 to 0.9992 is provided in Table 5. Good (%RSD) shows the repeatability of the method exhibiting robustness as shown by the inter-day and intra-day correctness range of 2.2 to 5.4, 2.3 to 5.5 and 4.4 to 9.4 respectively. The lowest quantified concentration 0.6 $\mu\text{g g}^{-1}$ (LOD) was determined using the equation

$3S_b/m$ with the standard deviation of the intercept represented as S_b and the calibration graph slope as m . The LOQ (Limit of Quantitation) ranged from 2.1 to $10.1 \mu\text{g g}^{-1}$ for the two calibration graphs was calculated using the equation $10S_b/m$. All calibration graphs exhibited a linear relationship between the LOD and the maximum concentration. Enrichment factor of the proposed system was deduced as 12, which is the result of ratio of microextraction (DES-LLME-SDIC) slope and that of the slope of the SDIC matrix match alone.

Table 5.

DES-LLME-SDIC Figures of Merit for Iodate Determination

Method	Regression Equation ^a	R ²	%RSD ^b		LOD ^c	LOQ ^d	LDR ^e	EF ^f
			Intra-day	Interday				
UV MATRIX	$y = 0.0143 (\pm 0.000257405) x$	0.9951	4.4	9.4	1.6	5.5	5.5-250	
MATCH	$+ 0.028 (\pm 0.007793312)$							
MATRIX MATCH	$y = 0.0008 (\pm 0.000005739) x$	0.9991	2.2	5.4	3.3	10.8	10.8-300	
SDIC	$+ 0.00167 (\pm 0.000868832)$							
DES-LLME	$y = 0.0095 (\pm 6.5595 \times 10^{-5}) x$	0.9992	2.3	5.5	0.6	2.1	2.1-50	12
SDIC	$+ 0.0045 (\pm 0.0019)$							

^a $R =$ the calculated slope of the graph ($\pm\text{SD}$) \times [iodate concentration to be determined (μM)] + the extrapolated y value (intercept) ($\pm\text{SD}$).

^b Relative standard deviation in percentile

^c The Lowest quantified concentration of the method ($\mu\text{g g}^{-1}$).

^d The Limit of quantitation of the method ($\mu\text{g g}^{-1}$).

^e Yielded Linear relationship of the method ($\mu\text{g g}^{-1}$).

^f Improvement factor: DES-LLME-SDIC/SDIC derived ratio.

Determined Concentrations of the Iodized Table Salt Samples

Concentration of the different iodized table salt samples was calculated using the slope and intercept of the two plotted calibration graphs together with the volume of the total sample solution, the dilution factor, and the molar mass (Mr) of the analyte ($\text{IO}_3^- = 173 \text{ g/mol}$).

By using the absorbance values obtained for the different salt samples, their concentration was calculated in micro moles per liter ($\mu\text{M L}^{-1}$) and subsequently micro grams per grams ($\mu\text{g g}^{-1}$).

Concentration in $\mu\text{M L}^{-1} = \text{absorbance plus intercept of the calibration graph divided by the slope.}$

Concentration in $\mu\text{g g}^{-1} = \text{concentration in micro mole per liter multiplied by the volume of the total sample solution, multiplied by the molar mass of the iodate standard, all divided by two and multiplied by the dilution factor.}$

$$\text{Concentration } \mu\text{g g}^{-1} = \text{concentration } (\mu\text{M g}^{-1}) \times \text{Volume} \times \text{Molar mass} / 2 * \text{DF}$$

From the table (table 6) it can be seen that both matrix calibration in absorbance measurement of the iodized salt samples gave comparable results indicated by the comparable concentrations found.

Table 6.

Determined Concentration of the Iodized Table Salt Samples

	TS1	TS2	TS3	TS4	TS5
DESLLMESDIC	5.91 ± 0.008	5.72 ± 0.015	5.72 ± 0.035	5.78 ± 0.021	5.74 ± 0.013
UV MATRIX	5.48 ± 0.08	5.36 ± 0.015	5.30 ± 0.035	5.37 ± 0.021	5.31 ± 0.013
MATCH					

TS1 to TS5 = Table salt Sample 1 to Table Salt Sample 5 ($\mu\text{g g}^{-1}$)

Evaluation of the Developed Method to other Techniques

A spectrophotometric technique (UV-Vis) was employed to independently verify the correctness of the suggested approach. In terms of LOD, LOQ, R^2 and %RSD, the performance of both methods was comparable considering that microextraction was involved in SDIC. However, it can be observed that the proposed green technique is Much cheaper than the UV-Vis technique.

Comparative evaluations of sensitivity, analysis time, reproducibility, and linearity were performed for iodate analysis in table salt to other methods described in the literature. The primary benefit of the suggested DES-LLME-SDIC approach over the alternatives is its simplicity, speed, and relatively inexpensiveness. Total analysis time of 14 minutes, including weighing, dissolution, redoxing, microextraction, and detection, demonstrated that the proposed approach was quicker than the majority of procedures described in the scientific literature. In terms of sensitivity, the proposed method was comparable in value to the ion chromatography technique by (Kumar et al., 2001) but quite less when compared to the method described by (Wang et al., 2009) (capillary zone electrophoresis), and that illustrated by (Xie et al., 2019) gas chromatography thermal conductivity detection.

However, it can be noted that these methods necessitate significant monetary investment and require tedious processes and in-depth experience.

Table 7.

Evaluation of the Developed Method to other Methods

Technique used ^a	Method Time (min)	LOD ^b ($\mu\text{g g}^{-1}$)	LOQ ^c ($\mu\text{g g}^{-1}$)	R ²	%RSD ^d	Ref.
Gas Chromatography TCD	40	0.014	0.047	0.9990	1.09-2.69	Xie et al., 2019
Capillary Zone electrophoresis	7	0.0035	0.012	0.9993	1.08-2.25	Wang et al., 2009
Spectrophotometric flow Injection analysis	-	0.02 (mg/l)	0.1-3.0 (mg/l)	0.9992	-	Shabani et al., 2011
Ion Chromatography	16	0.5	1.67	-	-	Kumar et al., 2001
UV-VIS	7	1.6	5.5	0.9951	4.4	This Study
DES-LLME-SDIC	14	0.6	2.1	0.9992	2.3	This Study

a TCD - thermal conductivity detection

b Lowest determined concentration.

c Lowest concentration tolerated with bias of the method

d Relative standard deviation in percentile.

CHAPTER V

CONCLUSIONS AND RECOMMENDATIONS

In this study, unique and convenient detection system was significantly improved in terms of its specificity and selectivity by liquid-liquid microextraction coupled with a green-approach extraction solvent. The combined extraction method (DES-LLME) and detection technique (SDIC) was used in this study to demonstrate their suitability and applicability to food samples (table salt).

Iodate in table salt was successfully quantified by DES-LLME as shown by the comparable result, after performing the redox reaction, followed by detection with SDIC.

Conclusions drawn from this study are that key parameters of simple unique detection systems such as SDIC are improved by microextraction techniques utilizing small volumes of environmentally friendly solvents such as deep eutectic solvents, reducing reliance on toxic organic solvents. This study proves such a system can be quantitatively employed for the determination of analytes of interest.

With major advantages such as speed, ease of use, portability, simplicity, and non-reliance on electricity, SDIC has demonstrated to be a formidable option for high-end complex systems, particularly for under-funded institutions, laboratories, and industries in emerging regions.

REFERENCES

- Abbott, A. P., Barron, J. C., Frisch, G., Gurman, S., Ryder, K. S., & Fernando Silva, A. (2011). Double layer effects on metal nucleation in deep eutectic solvents [10.1039/C0CP02244F]. *Physical Chemistry Chemical Physics*, 13(21), 10224-10231. <https://doi.org/10.1039/C0CP02244F>
- Abbott, A. P., Capper, G., Davies, D. L., Rasheed, R. K., & Tambyrajah, V. (2003). Novel solvent properties of choline chloride/urea mixtures [10.1039/B210714G]. *Chemical Communications*(1), 70-71. <https://doi.org/10.1039/B210714G>
- Abranches, D. O., Silva, L. P., Martins, M. A. R., Pinho, S. P., & Coutinho, J. A. P. (2020). Understanding the Formation of Deep Eutectic Solvents: Betaine as a Universal Hydrogen Bond Acceptor. *ChemSusChem*, 13(18), 4916-4921. <https://doi.org/10.1002/cssc.202001331>
- Al-Nidawi, M., & Alshana, U. (2021). Reversed-phase switchable-hydrophilicity solvent liquid-liquid microextraction of copper prior to its determination by smartphone digital image colorimetry. *Journal of Food Composition and Analysis*, 104, 104140. <https://doi.org/https://doi.org/10.1016/j.jfca.2021.104140>
- Alothman, Z. A., Habila, M. A., Yilmaz, E., Alabdulkarem, E. A., & Soylak, M. (2020). A novel deep eutectic solvent microextraction procedure for enrichment, separation and atomic absorption spectrometric determination of palladium at ultra-trace levels in environmental samples. *Measurement*, 153, 107394. <https://doi.org/https://doi.org/10.1016/j.measurement.2019.107394>
- Alshana, U., & Soylak, M. (2021). 18 - Deep eutectic solvents in microextraction. In R. Lucena & S. Cárdenas (Eds.), *Analytical Sample Preparation With Nano- and Other High-Performance Materials* (pp. 471-512). Elsevier. <https://doi.org/https://doi.org/10.1016/B978-0-12-822139-6.00019-5>
- Andersson, M., De Benoist, B., Darnton-Hill, I., & Delange, F. (2007). *Iodine deficiency in Europe: a continuing public health problem*. World Health Organization Geneva.
- Awuchi, C. G., Igwe, V. S., & Amagwula, I. O. (2020). Nutritional diseases and nutrient toxicities: A systematic review of the diets and nutrition for prevention and treatment. *International Journal of Advanced Academic Research*, 6(1), 1-46.
- Azizi, F., Aminorroya, A., Hedayati, M., Rezvanian, H., Amini, M., & Mirmiran, P. (2003). Urinary iodine excretion in pregnant women residing in areas with adequate iodine intake. *Public Health Nutrition*, 6(1), 95-98. <https://doi.org/10.1079/PHN2002366>
- Brough, L. (2021). Iodine Intake for Pregnant and Breastfeeding Women and Their

Infants Remains a Global Concern. In *J Nutr* (Vol. 151, pp. 3604-3605).
<https://doi.org/10.1093/jn/nxab364>

- Caleb, J., & Alshana, U. (2021). Supramolecular solvent-liquid-liquid microextraction followed by smartphone digital image colorimetry for the determination of curcumin in food samples. *Sustainable Chemistry and Pharmacy*, 21, 100424.
<https://doi.org/https://doi.org/10.1016/j.scp.2021.100424>
- Caleb, J., Alshana, U., & Ertaş, N. (2021). Smartphone digital image colorimetry combined with solidification of floating organic drop-dispersive liquid-liquid microextraction for the determination of iodate in table salt. *Food Chemistry*, 336, 127708. <https://doi.org/https://doi.org/10.1016/j.foodchem.2020.127708>
- Cappuccio, F. P. (2013). Cardiovascular and other effects of salt consumption. *Kidney Int Suppl* (2011), 3(4), 312-315. <https://doi.org/10.1038/kisup.2013.65>
- Clydesdale, F. (1978). Colorimetry—Methodology and Applications. *CRC critical reviews in food science and nutrition*, 10, 243-301.
<https://doi.org/10.1080/10408397809527252>
- Coskun, A., Wong, J., Khodadadi, D., Nagi, R., Tey, A., & Ozcan, A. (2012). A personalized food allergen testing platform on a cellphone. *Lab on a chip*, 13. <https://doi.org/10.1039/c2lc41152k>
- Cunha, S. C., & Fernandes, J. O. (2018). Extraction techniques with deep eutectic solvents. *TrAC Trends in Analytical Chemistry*, 105, 225-239.
<https://doi.org/https://doi.org/10.1016/j.trac.2018.05.001>
- Dahl, L., Johansson, L., Julshamn, K., & Meltzer, H. M. (2004). The iodine content of Norwegian foods and diets. *Public Health Nutrition*, 7(4), 569-576.
<https://doi.org/10.1079/phn2003554>
- Delange, F. (2001). Iodine deficiency as a cause of brain damage. *Postgraduate Medical Journal*, 77(906), 217. <https://doi.org/10.1136/pmj.77.906.217>
- Eckhoff, K. S. (1997). *Journal of Scientific Computing*, 12(2), 119-138.
<https://doi.org/10.1023/a:1025617731306>
- El Achkar, T., Greige-Gerges, H., & Fourmentin, S. (2021). Basics and properties of deep eutectic solvents: a review. *Environmental Chemistry Letters*, 19(4), 3397-3408. <https://doi.org/10.1007/s10311-021-01225-8>
- Fan, Y. J., Li, J. W., Guo, Y. P., Xie, L. W., & Zhang, G. (2021). Digital image colorimetry on smartphone for chemical analysis: A review. *Measurement*, 171, Article 108829. <https://doi.org/10.1016/j.measurement.2020.108829>
- Farebrother, J., Zimmermann, M. B., & Andersson, M. (2019). Excess iodine intake: sources, assessment, and effects on thyroid function. *Ann N Y Acad Sci*, 1446(1), 44-65. <https://doi.org/10.1111/nyas.14041>

- Fernández-Sánchez, L. M., Bermejo-Barrera, P., Fraga-Bermudez, J. M., Szpunar, J., & Lobinski, R. (2007). Determination of iodine in human milk and infant formulas. *Journal of Trace Elements in Medicine and Biology*, *21*, 10-13. <https://doi.org/https://doi.org/10.1016/j.jtemb.2007.09.006>
- Firdaus, M., Alwi, W., Trinoveldi, F., Rahayu, I., Rahmidar, L., & Warsito, K. (2014). Determination of Chromium and Iron Using Digital Image-based Colorimetry. *Procedia Environmental Sciences*, *20*, 298–304. <https://doi.org/10.1016/j.proenv.2014.03.037>
- Florindo, C., Branco, L. C., & Marrucho, I. M. (2019). Quest for Green-Solvent Design: From Hydrophilic to Hydrophobic (Deep) Eutectic Solvents. *ChemSusChem*, *12*(8), 1549-1559. <https://doi.org/10.1002/cssc.201900147>
- Florindo, C., Romero, L., Rintoul, I., Branco, L. C., & Marrucho, I. M. (2018). From Phase Change Materials to Green Solvents: Hydrophobic Low Viscous Fatty Acid-Based Deep Eutectic Solvents. *ACS Sustainable Chemistry & Engineering*, *6*(3), 3888-3895. <https://doi.org/10.1021/acssuschemeng.7b04235>
- Fuge, R. (2013). Soils and iodine deficiency. *Essentials of medical geology: revised edition*, 417-432.
- Golumbic, C. (1951). Liquid-Liquid Extraction Analysis. *Analytical Chemistry*, *23*(9), 1210-1217. <https://doi.org/10.1021/ac60057a004>
- Gupta, M., Pillai, A. K. K. V., Singh, A., Jain, A., & Verma, K. K. (2011). Salt-assisted liquid-liquid microextraction for the determination of iodine in table salt by high-performance liquid chromatography-diode array detection. *Food Chemistry*, *124*(4), 1741-1746. <https://doi.org/https://doi.org/10.1016/j.foodchem.2010.07.116>
- Gutiérrez, M. C., Ferrer, M. L., Mateo, C. R., & del Monte, F. (2009). Freeze-Drying of Aqueous Solutions of Deep Eutectic Solvents: A Suitable Approach to Deep Eutectic Suspensions of Self-Assembled Structures. *Langmuir*, *25*(10), 5509-5515. <https://doi.org/10.1021/la900552b>
- Hansen, B. B., Spittle, S., Chen, B., Poe, D., Zhang, Y., Klein, J. M., . . . Sangoro, J. R. (2021). Deep Eutectic Solvents: A Review of Fundamentals and Applications. *Chemical Reviews*, *121*(3), 1232-1285. <https://doi.org/10.1021/acs.chemrev.0c00385>
- Hassanien, M. H., Hussein, L. A., Robinson, E. N., & Preston Mercer, L. (2003). Human iodine requirements determined by the saturation kinetics model. *The Journal of Nutritional Biochemistry*, *14*(5), 280-287. [https://doi.org/https://doi.org/10.1016/S0955-2863\(03\)00034-2](https://doi.org/https://doi.org/10.1016/S0955-2863(03)00034-2)
- Hatch-McChesney, A., & Lieberman, H. R. (2022). Iodine and Iodine Deficiency: A Comprehensive Review of a Re-Emerging Issue. *Nutrients*, *14*(17). <https://doi.org/10.3390/nu14173474>

- Hatch-Mcchesney, A., & Lieberman, H. R. (2022). Iodine and Iodine Deficiency: A Comprehensive Review of a Re-Emerging Issue. *Nutrients*, *14*(17), 3474. <https://doi.org/10.3390/nu14173474>
- Huang, Z., Subhani, Q., Zhu, Z., Guo, W., & Zhu, Y. (2013). A single pump cycling-column-switching technique coupled with homemade high exchange capacity columns for the determination of iodate in iodized edible salt by ion chromatography with UV detection. *Food chemistry*, *139*(1-4), 144-148.
- Hussein Ael, A., Abbas, A. M., El Wakil, G. A., Elsamanoudy, A. Z., & El Aziz, A. A. (2012). Effect of chronic excess iodine intake on thyroid function and oxidative stress in hypothyroid rats. *Can J Physiol Pharmacol*, *90*(5), 617-625. <https://doi.org/10.1139/y2012-046>
- Ismail, S., Abdullahi, A. B., Alshana, U., & Ertaş, N. (2022). Switchable-hydrophilicity solvent liquid-liquid microextraction combined with smartphone digital image colorimetry for the determination of palladium in catalytic converters. *Analytical Sciences*. <https://doi.org/10.1007/s44211-022-00204-5>
- Jain, R., Jha, R. R., Kumari, A., & Khatri, I. (2021). Dispersive liquid-liquid microextraction combined with digital image colorimetry for paracetamol analysis. *Microchemical Journal*, *162*, 105870. <https://doi.org/https://doi.org/10.1016/j.microc.2020.105870>
- Jia, L., Huang, X., Zhao, W., Wang, H., & Jing, X. (2020). An effervescence tablet-assisted microextraction based on the solidification of deep eutectic solvents for the determination of strobilurin fungicides in water, juice, wine, and vinegar samples by HPLC. *Food Chemistry*, *317*, 126424. <https://doi.org/https://doi.org/10.1016/j.foodchem.2020.126424>
- Jiskra, J., Fait, T., Bílek, R., Krátký, J., Bartáková, J., Lukáš, J., . . . Potluková, E. (2014). Mild iodine deficiency in women after spontaneous abortions living in an iodine-sufficient area of Czech Republic: prevalence and impact on reproductive health. *Clinical endocrinology*, *80*(3), 452-458.
- Jooste, P. L., & Strydom, E. (2010). Methods for determination of iodine in urine and salt. *Best Practice & Research Clinical Endocrinology & Metabolism*, *24*(1), 77-88. <https://doi.org/https://doi.org/10.1016/j.beem.2009.08.006>
- Karimi, M., Dadfarnia, S., Shabani, A. M. H., Tamaddon, F., & Azadi, D. (2015). Deep eutectic liquid organic salt as a new solvent for liquid-phase microextraction and its application in ligandless extraction and preconcentration of lead and cadmium in edible oils. *Talanta*, *144*, 648-654. <https://doi.org/https://doi.org/10.1016/j.talanta.2015.07.021>
- Khazan, M., Azizi, F., & Hedayati, M. (2013). *A Review on Iodine Determination Methods in Salt and Biological Samples*. <https://doi.org/10.5812/scimetr.14092>

- Kovač, M. J., Jokić, S., Jerković, I., & Molnar, M. (2022). Optimization of Deep Eutectic Solvent Extraction of Phenolic Acids and Tannins from *Alchemilla vulgaris* L. *Plants*, *11*(4), 474. <https://doi.org/10.3390/plants11040474>
- Kulkarni, P. S., Dhar, S. D., & Kulkarni, S. D. (2013). A rapid assessment method for determination of iodate in table salt samples. *Journal of Analytical Science and Technology*, *4*(1), 21. <https://doi.org/10.1186/2093-3371-4-21>
- Kumar, A., Srivastava, D. N., Chau, T. T. M., Long, H. D., Bal, C., Chandra, P., . . . Bandopadhyaya, G. P. (2007). Inoperable Hepatocellular Carcinoma: Transarterial ¹⁸⁸Re HDD-Labeled Iodized Oil for Treatment—Prospective Multicenter Clinical Trial. *Radiology*, *243*(2), 509-519. <https://doi.org/10.1148/radiol.2432051246>
- Kumar, S. D., Maiti, B., & Mathur, P. K. (2001). Determination of iodate and sulphate in iodized common salt by ion chromatography with conductivity detection. *Talanta*, *53*(4), 701-705. [https://doi.org/https://doi.org/10.1016/S0039-9140\(00\)00504-X](https://doi.org/https://doi.org/10.1016/S0039-9140(00)00504-X)
- Leung, A. M., & Braverman, L. E. (2014). Consequences of excess iodine. *Nature Reviews Endocrinology*, *10*(3), 136-142. <https://doi.org/10.1038/nrendo.2013.251>
- Liu, Y., Friesen, J. B., McAlpine, J. B., Lankin, D. C., Chen, S.-N., & Pauli, G. F. (2018). Natural Deep Eutectic Solvents: Properties, Applications, and Perspectives. *Journal of Natural Products*, *81*(3), 679-690. <https://doi.org/10.1021/acs.jnatprod.7b00945>
- Lu, W., Liu, S., & Wu, Z. (2022). Recent Application of Deep Eutectic Solvents as Green Solvent in Dispersive Liquid-Liquid Microextraction of Trace Level Chemical Contaminants in Food and Water. *Critical Reviews in Analytical Chemistry*, *52*(3), 504-518. <https://doi.org/10.1080/10408347.2020.1808947>
- Mathews, D. M., Johnson, N. P., Sim, R. G., O'Sullivan, S., Peart, J. M., & Hofman, P. L. (2021). Iodine and fertility: do we know enough? *Hum Reprod*, *36*(2), 265-274. <https://doi.org/10.1093/humrep/deaa312>
- Niwattisaiwong, S., Burman, K. D., & Li-Ng, M. (2017). Iodine deficiency: Clinical implications. *Cleve Clin J Med*, *84*(3), 236-244.
- Obregon, M.-J., Del Rey, F. E., & De Escobar, G. M. (2005). The Effects of Iodine Deficiency on Thyroid Hormone Deiodination. *Thyroid*, *15*(8), 917-929. <https://doi.org/10.1089/thy.2005.15.917>
- Ortega-Zamora, C., González-Sálamo, J., & Hernández-Borges, J. (2021). Deep Eutectic Solvents Application in Food Analysis. *Molecules*, *26*(22), 6846. <https://doi.org/10.3390/molecules26226846>
- Paiva, A., Craveiro, R., Aroso, I., Martins, M., Reis, R. L., & Duarte, A. R. C. (2014). Natural Deep Eutectic Solvents – Solvents for the 21st Century. *ACS*

Sustainable Chemistry & Engineering, 2(5), 1063-1071.
<https://doi.org/10.1021/sc500096j>

- Pena-Pereira, F., & Namieśnik, J. (2014). Ionic Liquids and Deep Eutectic Mixtures: Sustainable Solvents for Extraction Processes. *ChemSusChem*, 7(7), 1784-1800. <https://doi.org/10.1002/cssc.201301192>
- Plastiras, O.-E., & Samanidou, V. (2022). Applications of Deep Eutectic Solvents in Sample Preparation and Extraction of Organic Molecules. *Molecules*, 27(22), 7699.
- Porto, I. S. A., Santos Neto, J. H., dos Santos, L. O., Gomes, A. A., & Ferreira, S. L. C. (2019). Determination of ascorbic acid in natural fruit juices using digital image colorimetry. *Microchemical Journal*, 149, 104031.
<https://doi.org/https://doi.org/10.1016/j.microc.2019.104031>
- Reichardt, C. (1994). Solvatochromic dyes as solvent polarity indicators. *Chemical reviews*, 94(8), 2319-2358.
- Rodríguez-Llorente, D., Cañada-Barcala, A., Álvarez-Torrellas, S., Águeda, V. I., García, J., & Larriba, M. (2020). A Review of the Use of Eutectic Solvents, Terpenes and Terpenoids in Liquid-liquid Extraction Processes. *Processes*, 8(10), 1220. <https://doi.org/10.3390/pr8101220>
- Ruß, C., & König, B. (2012). Low melting mixtures in organic synthesis – an alternative to ionic liquids? *Green Chemistry*, 14(11), 2969.
<https://doi.org/10.1039/c2gc36005e>
- Saha, A., Mukherjee, S., Bhattacharjee, A., Sarkar, D., Chakraborty, A., Banerjee, A., & Chandra, A. K. (2019). Excess iodine-induced lymphocytic impairment in adult rats. *Toxicology Mechanisms and Methods*, 29(2), 110-118.
<https://doi.org/10.1080/15376516.2018.1528647>
- Shabani, A. M. H., Ellis, P. S., & McKelvie, I. D. (2011). Spectrophotometric determination of iodate in iodised salt by flow injection analysis. *Food chemistry*, 129(2), 704-707.
- Silva, R., Oliveira, A. F., & Neves, E. (1998). Spectrophotometric Determination of Iodate in Table Salt. *Journal of the Brazilian Chemical Society*, 9, 171-174.
<https://doi.org/10.1590/S0103-50531998000200009>
- Smith, E. L., Abbott, A. P., & Ryder, K. S. (2014). Deep Eutectic Solvents (DESs) and Their Applications. *Chemical Reviews*, 114(21), 11060-11082.
<https://doi.org/10.1021/cr300162p>
- Sánchez-Condado, A., Carriedo, G. A., Presa Soto, A., Rodríguez-Álvarez, M. J., García-Álvarez, J., & Hevia, E. (2019). Organolithium-Initiated Polymerization of Olefins in Deep Eutectic Solvents under Aerobic Conditions. *ChemSusChem*, 12(13), 3134-3143.
<https://doi.org/10.1002/cssc.201900533>

- Tang, B., & Row, K. H. (2013). Recent developments in deep eutectic solvents in chemical sciences. *Monatshefte für Chemie - Chemical Monthly*, 144(10), 1427-1454. <https://doi.org/10.1007/s00706-013-1050-3>
- Trumbo, P. R. (2016). FDA regulations regarding iodine addition to foods and labeling of foods containing added iodine. *The American Journal of Clinical Nutrition*, 104(suppl_3), 864S-867S. <https://doi.org/10.3945/ajcn.115.110338>
- Van Osch, D. J. G. P., Parmentier, D., Dietz, C. H. J. T., Van Den Bruinhorst, A., Tuinier, R., & Kroon, M. C. (2016). Removal of alkali and transition metal ions from water with hydrophobic deep eutectic solvents. *Chemical Communications*, 52(80), 11987-11990. <https://doi.org/10.1039/c6cc06105b>
- van Osch, D. J. G. P., Zubeir, L. F., van den Bruinhorst, A., Rocha, M. A. A., & Kroon, M. C. (2015). Hydrophobic deep eutectic solvents as water-immiscible extractants [10.1039/C5GC01451D]. *Green Chemistry*, 17(9), 4518-4521. <https://doi.org/10.1039/C5GC01451D>
- Wang, Y., Zhang, Z., Ge, P., Wang, Y., & Wang, S. (2009). Iodine deficiency disorders after a decade of universal salt iodization in a severe iodine deficiency region in China. *Indian Journal of Medical Research*, 130(4).
- World Health, O. (2007). Assessment of iodine deficiency disorders and monitoring their elimination: a guide for programme managers.
- World Health, O. (2013). *Urinary iodine concentrations for determining iodine status in populations*.
- Xie, Z., & Zhao, J. (2004). Reverse flow injection spectrophotometric determination of iodate and iodide in table salt. *Talanta*, 63(2), 339-343. <https://doi.org/https://doi.org/10.1016/j.talanta.2003.10.050>
- Xu, H., Peng, J., Kong, Y., Liu, Y., Su, Z., Li, B., . . . Tian, W. (2020). Key process parameters for deep eutectic solvents pretreatment of lignocellulosic biomass materials: A review. *Bioresource Technology*, 310, 123416. <https://doi.org/https://doi.org/10.1016/j.biortech.2020.123416>
- Yilmaz, E., & Soylak, M. (2020). 15 - Functionalized nanomaterials for sample preparation methods. In C. Mustansar Hussain (Ed.), *Handbook of Nanomaterials in Analytical Chemistry* (pp. 375-413). Elsevier. <https://doi.org/https://doi.org/10.1016/B978-0-12-816699-4.00015-3>
- Yue, X., Cao, Y., Wang, Y., Bao, H., & Xu, Y. (2022). Optimization of Deep Eutectic Solvents Extraction of Effective Components from Phellodendron chinense Schneid by Response Surface Methodology. *International Journal of Chemical Engineering*, 2022, 1-12. <https://doi.org/10.1155/2022/3881551>
- Zahrina, I., Nasikin, M., & Mulia, K. (2017). Evaluation of the interaction between molecules during betaine monohydrate-organic acid deep eutectic mixture formation. *Journal of Molecular Liquids*, 225, 446-450.

<https://doi.org/https://doi.org/10.1016/j.molliq.2016.10.134>

- Zeng, H., Qiao, K., Li, X., Yang, M., Zhang, S., Lu, R., . . . Zhou, W. (2017). Dispersive liquid–liquid microextraction based on the solidification of deep eutectic solvent for the determination of benzoylureas in environmental water samples. *Journal of separation science*, *40*(23), 4563-4570.
- Zhang, Q., De Oliveira Vigier, K., Royer, S., & Jérôme, F. (2012). Deep eutectic solvents: syntheses, properties and applications [10.1039/C2CS35178A]. *Chemical Society Reviews*, *41*(21), 7108-7146.
<https://doi.org/10.1039/C2CS35178A>
- Zhang, Z., Wang, H., Chen, Z., Wang, X., Choo, J., & Chen, L. (2018). Plasmonic colorimetric sensors based on etching and growth of noble metal nanoparticles: Strategies and applications. *Biosensors and Bioelectronics*, *114*, 52-65. <https://doi.org/https://doi.org/10.1016/j.bios.2018.05.015>
- Zhu, J., Xu, Y., Feng, X., & Zhu, X. (2018). A detailed study of physicochemical properties and microstructure of EmimCl-EG deep eutectic solvents: Their influence on SO₂ absorption behavior. *Journal of Industrial and Engineering Chemistry*, *67*, 148-155.
<https://doi.org/https://doi.org/10.1016/j.jiec.2018.06.025>
- Zimmermann, M. B. (2009). Iodine deficiency. *Endocr Rev*, *30*(4), 376-408.
<https://doi.org/10.1210/er.2009-0011>
- Zimmermann, M. B., Jooste, P. L., & Pandav, C. S. (2008). Iodine-deficiency disorders. *The Lancet*, *372*(9645), 1251-1262.
[https://doi.org/https://doi.org/10.1016/S0140-6736\(08\)61005-3](https://doi.org/https://doi.org/10.1016/S0140-6736(08)61005-3)

ORIGINALITY REPORT

27%

SIMILARITY INDEX

23%

INTERNET SOURCES

22%

PUBLICATIONS

17%

STUDENT PAPERS

PRIMARY SOURCES

1	docs.neu.edu.tr Internet Source	2%
2	Submitted to Yakın Doğu Üniversitesi Student Paper	1%
3	theses.hal.science Internet Source	1%
4	pubs.rsc.org Internet Source	1%
5	www.mdpi.com Internet Source	1%
6	icabc2020.firat.edu.tr Internet Source	1%
7	Submitted to Indian Institute of Technology Guwahati Student Paper	1%
8	Submitted to Nottingham Trent University Student Paper	1%
9	Submitted to Taylor's Education Group Student Paper	1%